

Article

# Beyond Site Detection: The Role of Satellite Remote Sensing in Analysing Archaeological Problems. A Case Study in Lithic Resource Procurement in the Atacama Desert, Northern Chile

César Borie <sup>1,\*</sup>, César Parcero-Oubiña <sup>2</sup>, Youngsang Kwon <sup>3</sup>, Diego Salazar <sup>4</sup>, Carola Flores <sup>5</sup>, Laura Olguín <sup>6</sup> and Pedro Andrade <sup>7</sup>

<sup>1</sup> Programa de Doctorado en Antropología UCN-UTA, Universidad Católica del Norte, Calle R.P. Gustavo Le Paige 380, San Pedro de Atacama, 1410000 Antofagasta, Chile. CONICYT-PCHA/Doctorado Nacional/2015-21150953. FONDECYT 1151203

<sup>2</sup> Instituto de Ciencias del Patrimonio (Incipit), Consejo Superior de Investigaciones Científicas (CSIC), Av. de Vigo, 15705 Santiago de Compostela, Spain; cesar.parcero-oubina@incipit.csic.es

<sup>3</sup> Earth Sciences Department, University of Memphis, Memphis, 109 Johnson Hall, Memphis, TN 38152, USA; ykwon@memphis.edu

<sup>4</sup> Departamento de Antropología, Facultad de Ciencias Sociales, Universidad de Chile, Ignacio Carrera Pinto 1045, Núñoa, 7800284 Santiago, Chile. FONDECYT 1151203; dsalazar@uchile.cl

<sup>5</sup> Centro de Estudios Avanzados en Zonas Áridas (CEAZA), Ossandón 877, 1781681 Coquimbo, Chile. FONDECYT 3170913, 1151203; carola.flores@ceaza.cl

<sup>6</sup> Programa de Doctorado en Antropología UCN-UTA, Universidad Católica del Norte, Calle R.P. Gustavo Le Paige 380, San Pedro de Atacama, 1410000 Antofagasta, Chile. FONDECYT 1151203; olguinlaura.o@gmail.com

<sup>7</sup> Carrera de Antropología, Universidad de Concepción, Víctor Lamas 1290, 4070386 Concepción, Chile. FONDECYT 1151203; pandradem@udec.cl

\* Correspondence: cbc032@alumnos.ucn.cl

Received: 28 February 2019; Accepted: 5 April 2019; Published: 10 April 2019



**Abstract:** Remote sensing archaeology in recent years has emphasized the use of high-precision and high-accuracy tools to achieve the detailed documentation of archaeological elements (drones, LIDAR, etc.). Satellite remote sensing has also benefited from an increase in the spatial and spectral resolution of the sensors, which is enabling the discovery and documentation of new archaeological features and sites worldwide. While there can be no doubt that a great deal is being gained via such “site detection” approaches, there still remains the possibility of further exploring remote sensing methods to analyse archaeological problems. In this paper, this issue is discussed by focusing on one common archaeological topic: the mapping of environmental resources used in the past and, in particular, the procurement of lithic raw material by hunter-gatherer groups. This is illustrated by showing how the combined use of Landsat 8 images and “ground-truthing” via focused field studies has allowed the identification of a number of potential chert sources, the major lithic resource used by coastal groups between 11,500–1,500 cal. BP, in a vast area of the Atacama Desert covering 22,500 km<sup>2</sup>. Besides discussing the case study, the strength of remote sensing techniques in addressing archaeological questions comprising large spatial scales is highlighted, stressing the key role they can play in the detection and study of specific environmental resources within challenging physical settings.

**Keywords:** archaeology; arid environments; satellite remote sensing; lithological mapping; lithic procurement; chert sourcing; Landsat 8; GIS

## 1. Introduction

Remote sensing in archaeology has grown into a large and varied field. In particular, satellite remote sensing has benefited from an increase in the spatial and spectral resolution of the sensors, an improvement which has enabled the discovery and documentation of new archaeological features and sites worldwide [1–3]. While there can be no doubt that a great deal can be gained from these “site detection” approaches, there is still potential to be explored in using remote sensing methods as tools to analyse archaeological problems, especially on large geographical scales. In this paper, this potential is discussed by focusing on one common archaeological topic: the mapping of environmental resources used in the past, and in particular, the procurement of lithic raw material by ancient hunter-gatherer groups.

Since the 1970s, geological studies have tested the capacity of satellite remote sensing for lithological mapping in different environmental contexts, highlighting the ability of spectral analysis to discriminate between diverse rock and soil units, thus complementing and improving the accuracy of the data provided by conventional geological maps [4–9]. On the other hand, archaeologists have long emphasized the technological and social importance of high-quality rocks for prehistoric hunter-gatherer societies [10–14]. The large geographical ranges involved in the direct or indirect procurement of such rocks and their consistent use over long time spans imply that approaches on regional or landscape-based scales are especially well-suited for tackling these questions [15–18]. There seems to be a “natural” point of convergence here between the capabilities of satellite remote sensing and the research questions raised by some archaeological approaches. However, so far, these techniques have not received much attention from archaeologists concerned with the procurement of lithic resources in the past, despite the remarkable advantages they represent for addressing this problem on large spatial scales [19–22].

In this paper, following the trend of previous research [22], it is argued that satellite remote sensing in archaeology holds a great potential beyond the common (and indeed useful) aims of site detection. In particular, the suitability of remote sensing to overcome some of the major limitations of traditional archaeological methodologies is stressed. This is illustrated via a case study that shows how the combined use of freely accessible satellite images and “ground-truthing” through focused field studies has allowed the identification of a number of primary and secondary sources of chert in a vast area of the Atacama Desert covering 22,500 km<sup>2</sup>. This is a large-scale approach that takes full advantage of the natural conditions of the study area and also of the information contained in the “grey literature” provided by spatially discrete and dispersed CRM reports, offering a cost-effective methodology which can easily be replicated in other contexts.

The benefits and drawbacks of the methodology will be assessed, stressing the need for higher spectral resolution satellite imagery and “ground-truthing” via Visible Near-Infrared (VIS/NIR) and Fourier Transform Infrared (FTIR) reflectance spectroscopy for further refinement of the remote sensing approach, and also the need to conduct lithic provenance studies with a high level of geographical and geological resolution [23]. Finally, the strength of remote sensing techniques in addressing archaeological questions that comprise large spatial scales is discussed, and attention is drawn to the key role which they can play in the detection and study of specific environmental resources, such as lithic source areas, within challenging and poorly studied physical settings.

## 2. Satellite Remote Sensing in Problem-Oriented Research

Broadly speaking, and without any pretensions of being exhaustive, it could be argued that satellite images are used in archaeology in two possible ways: as exploratory tools (aimed at prospecting the landscape in order to find new sites or features of archaeological interest) or as part of problem-oriented research (as tools to answer explicit questions about the past). Although this broad-brush distinction is by no means new [22,24], it is not very clear: finding new archaeological places of interest can be problem-oriented research in itself, for instance, in the case of heritage management bodies, whose purpose is precisely to identify and document the highest number of

archaeological elements in any given area or region [25]. The difference does not imply any hierarchy at all; both approaches are equally useful and productive, at different levels and with different impacts. However, they usually imply a different approach to the use of satellite images and involve different methods and skills.

Exploratory analysis is commonly a general-purpose task, aimed at finding any elements of potential archaeological interest in a region. Consequently, the traces that are to be detected are equally varied (crop marks, soil marks, topographical anomalies, etc.). It follows almost naturally that general-purpose methods, such as visual photointerpretation, which do not require sophisticated processing of the remote sensing data to provide broad, and rather generic, results, are the best suited to such applications; on the contrary, any methods tailored to find certain specific proxies using more sophisticated image processing methods are typically not very good candidates for this [26,27].

It is by no means implied that all the aforementioned general-purpose applications do not involve any kind of expertise or skills [28]. The point to be noticed here is that, within these exploratory approaches, satellite images are typically used just like other types of aerial photos, for visual interpretation. Until recently, the medium to coarse spatial resolution of satellite imagery (especially when compared with aerial photos) strongly limited its use for visual prospection. Even now, despite the increasing availability of images with a higher spatial resolution (even those freely accessible through Google Maps, Bing Maps, and similar sites), it is still true that “satellite reconnaissance is better suited for mapping large-scale and broad landscape features such as paleochannels or detecting upstanding monuments in semi-arid environments, while airborne imaging remains the preferred approach for a detailed study of past geo-cultural activity” [29] (p.5).

In this paper, the focus is placed on the other main use of satellite imagery; spectral analysis. There are two main reasons which have limited the use of satellite spectral analysis in archaeology. Firstly, there is, again, an issue with the spatial resolution of most satellite imagery, which is insufficient to single out the marks of many individual archaeological features. The development of high-spatial resolution sensors has alleviated this limitation to some extent, although the limited spectral resolution of these spatially detailed sensors comes as an unavoidable drawback [22]. Secondly, and perhaps more importantly, there are no general-purpose methods for analysing the spectral information of satellite imagery, because this task is highly dependent on the characteristics of the specific target elements and on the characteristics of the surrounding landscape.

In any case, there are some good examples that prove that, when the conditions are right, remote sensing can fill relevant gaps in archaeological research. It is not surprising that the best examples of this synergy are those related to the delimitation of environmental variables which can be informative of economic or social practices in the past, especially those related to geological and soil mapping. As B. Vining pointed out a few years ago that “while environmental mapping was one of the earliest applications of archaeological remote sensing, the focus on site detection has shifted attention away from this area. Using spectral data to delimit environmental variables is the strong suite of remote sensing” [22] (p. 493). Different examples prove the usefulness of using satellite imagery for the analysis of environmental factors in relation to archaeological problems, such as the development of early agricultural practices [30]; the identification of patterns of settlements and paths [31]; or, similar to our case study, the detection of sources of raw stone material [32].

While such approaches might be equally feasible in any context, the existence of a good state of preservation and visibility of the archaeological evidence is always a factor that increases the chances of a successful remote sensing approach. In this respect, arid regions typically rank very high, since the absence of dense vegetation allows for a more direct observation of the properties of the soils. A first obvious benefit comes when satellite imagery is used for visual interpretation [33,34]. However, spectral analysis also benefits from the absence of dense vegetation. South America, or at least those large parts of it occupied by arid or semi-arid landscapes, represents a geographical context which can be especially suited to these kinds of approaches: the existence of large areas with very low population densities, both in the present and in historical times, implies a low amount of

human-induced alteration of the landscape, thus resulting in a reduced level of “noise” detectable through satellite images. Furthermore, many of these areas are geomorphologically very stable, an aspect which also increases the value of remote observation for the interpretation of past patterns. Finally, and more importantly, these largely unpopulated areas usually pose significant difficulties for traditional archaeological recognition due to their vastness, difficult access, and poor communication (which, for instance, limits the use of GPS and similar devices). All this suggests that spectral analysis of satellite imagery has great potential to be applied in many areas of arid and semi-arid South America, but at the moment, there are few examples of its application in the region [35], particularly if only those cases that go beyond the not-so-uncommon visual interpretation of satellite imagery are considered [36,37].

The increasing availability of free imagery represents a good opportunity to move forward and take advantage of the potential benefits of a problem-oriented use of satellite remote sensing in this region. The case study presented in the following sections attempts to illustrate this in practice.

### 3. Introduction to the Case Study: Research Problem and Background

#### 3.1. Lithic Procurement Strategies in Hunter-Gatherer Societies

Land-use patterns and, particularly, lithic procurement strategies, have long been major topics in the archaeological research of ancient hunter-gatherer societies [11–14,38,39]. In particular, the procurement of high-quality stone (the concept of high quality rocks, as it is used here, stands for the ease of a given lithic raw material for controlled knapping [14], and also for the functional requirements that the artefacts made of such raw material have to meet to achieve their intended use, for instance, in terms of edge strength, requirements that usually prompted the selection of cryptocrystalline toolstone like chert, chalcedony, flint, and jasper in prehistoric times [10,40]) has been considered a key aspect in the technological organization of these kinds of groups and an activity that affected, in diverse and complex ways, the configuration of their settlement and mobility patterns [13,39–41].

The geological occurrence of the most suitable rocks for tool manufacturing is manifested unevenly across the landscape, and there is normally a strong discordance between the spatial distribution of critical subsistence resources and these natural deposits of raw material [10,13,14,39]. Therefore, hunter-gatherer societies had to develop strategies to ensure the availability of adequate toolstone raw materials in the locations where they were required for subsistence activities [13,42,43], investing, in some cases, considerable time and effort in their procurement [12,13,44].

In desert areas such as the Atacama, this discordance is manifested as a stark contrast between the coastal environments, rich in biotic resources, where local hunter-gatherer-fisher communities settled, and the vast barren landscape of the Central Depression, profuse in high-quality lithic resources, where only ephemeral occupations were possible [45–50]. The technological organization of those communities relied heavily on high-quality non-local chert, which comprises between 83% and 95% of the coastal lithic assemblages documented for the period 11,500–1,500 cal. BP [51]. To sustain that, these groups had to organize forays taking them between 40–115 km away from their settlement areas into the hyper-arid core of the Atacama Desert [45,46,48,52–54].

Material evidence for these logistic forays is abundant but widely dispersed in the Atacama Central Depression, just like the chert-bearing geological formations [46,48,53,54]. This scenario imposes challenges for traditional archaeological methodologies, mainly due to the cost in time and human resources that the systematic study of these contexts demands and the extremely complex practical conditions for fieldwork.

In order to deal with these limitations, different research techniques need to be integrated in innovative ways, providing access to the cumulative and continuous expression of the lithic record across space on an appropriate geographical scale [15–18,40,42].

The Atacama Desert, and particularly its hyper-arid Central Depression, has been geologically stable since the end of the Pliocene [55–58]. In exchange for its challenging fieldwork conditions,

this stable, bare earth landscape, offers exceptional conditions for archaeological visibility and preservation, thus making it an ideal setting for the use of satellite remote sensing techniques [53].

### 3.2. Satellite Imagery and the Mapping of Lithic Source Areas

Among the multispectral satellite images available with global coverage and free access, those captured by the Landsat program sensors are among the most widely used in geology and archeology for lithological mapping [9]. Satellites from NASA's Landsat program have been in sun-synchronous orbit since 1972, capturing scenes from the earth's surface with a coverage of  $185 \times 185$  km per single image (USGS). Their sensors provide a moderate spatial and radiometric resolution, covering the visible and near-infrared (VNIR) range with a resolution of 15 to 60 m and also, from the Landsat 4-5 mission onwards, the Thermal Infrared (TIR) range with resolutions of 60 to 120 m.

The wide distribution of their bands in the electromagnetic spectrum makes Landsat images one of the most versatile tools for remote sensing studies in diverse landscape conditions [59]. The geological remote sensing community makes use of them extensively for lithological and mineralogical mapping, especially since the advent of the Landsat Thematic Mapper (TM) sensor [9], following the precept that reflectance characteristics of the different lithological classes (rocks or soil types) are primarily derived from the presence and relative proportion of their mineral components [60,61].

For lithological discrimination, specifically in zones with mineralogical alteration, Landsat bands are commonly combined in RGB composites and are subject to digital enhancement techniques, such as band-ratioing, principal component analysis (PCA), and supervised classification [9]. In general, bands within the visible to SWIR (or VNIR) range (0.4–2.3  $\mu\text{m}$ ) are selected for these tasks, due to the presence of diagnostic spectral features of certain minerals, such as clays, carbonates, and iron oxides, which allow zones with hydrothermally altered rocks to be differentiated from those with unaltered rocks [7,9,62].

Archaeological studies on local and regional scales have successfully exploited some of these enhancement techniques in Landsat images for the detection of ancient lithic source areas. A few examples can illustrate this. Carr and Turner [19], in a pioneering study within this line of research, combined field studies, laboratory analysis, and satellite remote sensing on Landsat 5 TM images to locate prehistoric quarries in the Horse Prairie region, in the southwest of Montana, United States. Using "ground truth" data provided by reflective spectroscopic analysis of field samples, these researchers identified distinctive spectral profiles for chert weathered outcrops and soils with dispersions of rocks extracted from these outcrops. The spectral data was incorporated into a supervised classification within which the adjacency of pixels assigned to these two types of deposition contexts proved to be indicative of the location of ancient chert quarries, which had previously been unknown [19].

More than a decade later, Rosendahl (2010) used Landsat 7 ETM+ VNIR bands for a principal component analysis, in conjunction with pedestrian surveys in the Troodos foothills, Cyprus, as training data for a supervised classification. This work identified potential chert-bearing areas within the Lefkara geological formation and was used for the design of targeted pedestrian surveys.

A more recent example is that of Cattáneo, et al. [63] who demonstrated the successful identification of potential prehistoric lithic sources using Landsat 7 VNIR bands in the northeast of the Province of Santa Cruz, in Argentina.

The aforementioned references seek to highlight the relevance and potential of the integration of satellite remote sensing tools for lithic landscape archaeological research. In the following section, the guidelines of a multidisciplinary research strategy benefitting from this integration for the reconstruction of the Southern Atacama prehistoric lithic landscape are detailed.

#### 4. Study Area: Physical and Archaeological Setting

The study area extends between  $24.6^{\circ}$  and  $26^{\circ}$  S, comprising the southern part of the Atacama Desert, and stretches from the Pacific coast to the foothills of the Andes, a transect of ca. 150 km. This area of  $22,500 \text{ km}^2$  lays within the southern portion of the Antofagasta region, Chile, and is characterized by a complete lack of perennial streams and great altitudinal contrast (Figure 1).

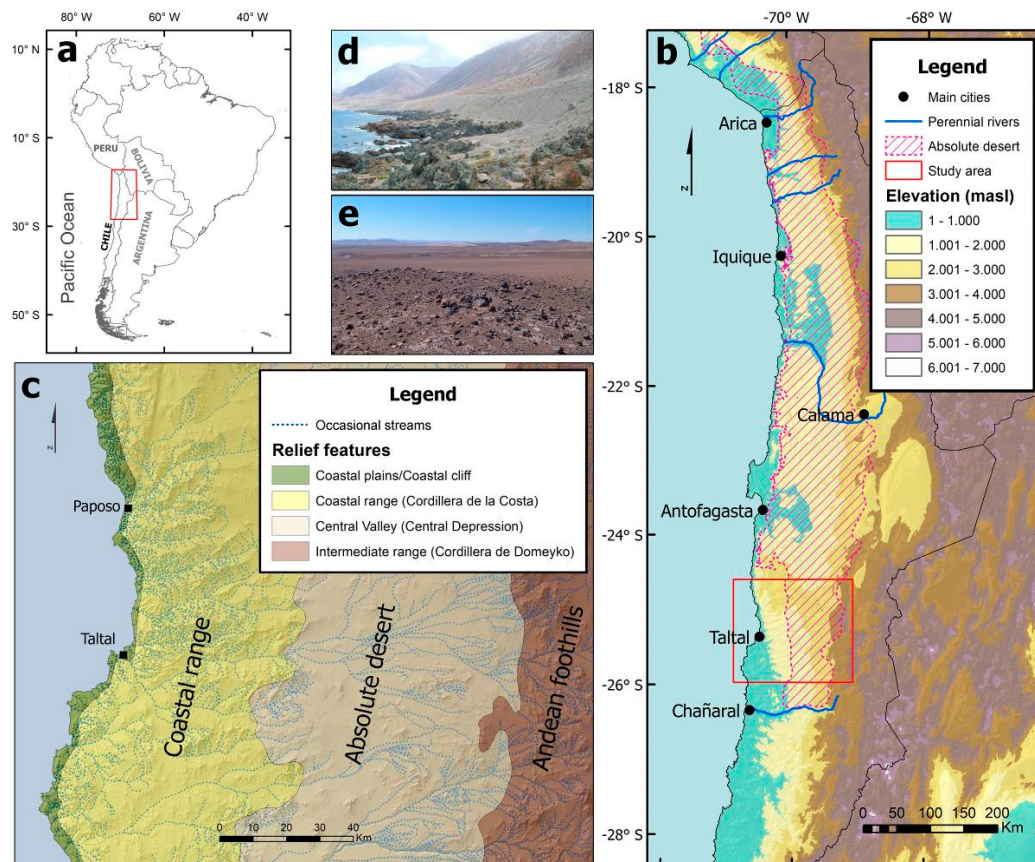


**Figure 1.** (a) Map of South America, red box indicates the extent of (b) altitudinal map showing the location of the absolute desert in northern Chile (hatched polygon), main cities (black dots), and perennial streams (blue lines). Red box in (b) corresponds to the map of study area (c) with the main topographic features and occasional streams (dashed blue lines); (d) panoramic view of the coastal platform and cliffs; (e) panoramic view of the absolute desert of Taltal.

The main relief features correspond to, from west to east, a narrow litoral platform, a steep coastal range (Cordillera de la Costa), a longitudinal central valley or Central Depression, the foothills of the Andes (represented in the area by the Cordillera de Domeyko) and, finally, the higher-level Andes and the Altiplano [64].

On the coast, facing the rich and diverse marine ecosystems of the Pacific [65], dense fogs sustain isolated plant communities of the *lomas* formation, which attract minor fauna species [66]. Fresh water is available from small springs along the litoral platform and in the neighboring coastal range, fed by occasional coastal rains related to ENSO events [67,68]. The cliff-like Cordillera de la Costa, with peaks of 2,000 m.a.s.l., blocks the eastward advance of the coastal fogs and, together with the cold oceanic Humbold Current and the rain-shadow effect of the Andes, intensifies the hyper-arid conditions of the Central Depression [55,69]. In this 70 km wide Central Valley, with its vast plains, isolated hills, and low-altitude ranges, rainfall averages less than 1 mm per year, solar radiation is extremely high, and strong thermal oscillations occur throughout the day [56,69]. Plant and animal communities are minimal here and are restricted to the scarce and widely scattered locations around groundwater

outcrops [70]. To the east, the streams and wetlands of the Cordillera de Domeyko and the upper Andes offer a relative abundance of water resources, animals, and plants [70].

The extreme and long-standing aridity of the Central Depression [55,56,69,71], except during phases of relatively more humid conditions [72–76], has always hindered stable human occupation. Accordingly, settlement patterns have historically been anchored to the coastal environments, which are richer in biotic resources [45,47,50,77,78].

Nevertheless, the vast wealth of high-quality rock in the Central Valley has attracted sporadic, but recurrent, occupations by the coastal inhabitants of the Atacama for over 10,000 years [45–48,52–54,78]. The abundance of sedimentary microcrystalline and cryptocrystalline silicates, or chert [79], throughout the area is explained by the presence of several spatially restricted hydrothermal alteration zones, which mainly developed in rocks of the Chile-Alemania Formation, part of a continental volcanic chain of the Palaeocene-Middle Eocene age [80]. Igneous rocks intrude this Formation (e.g., quartziferous, tonalitic, and granodioritic porphyries) and, due to the action of geothermal systems, they have gone through silicification, argillization, and propylitization processes of variable intensity and extension [80,81] (Figure 2).

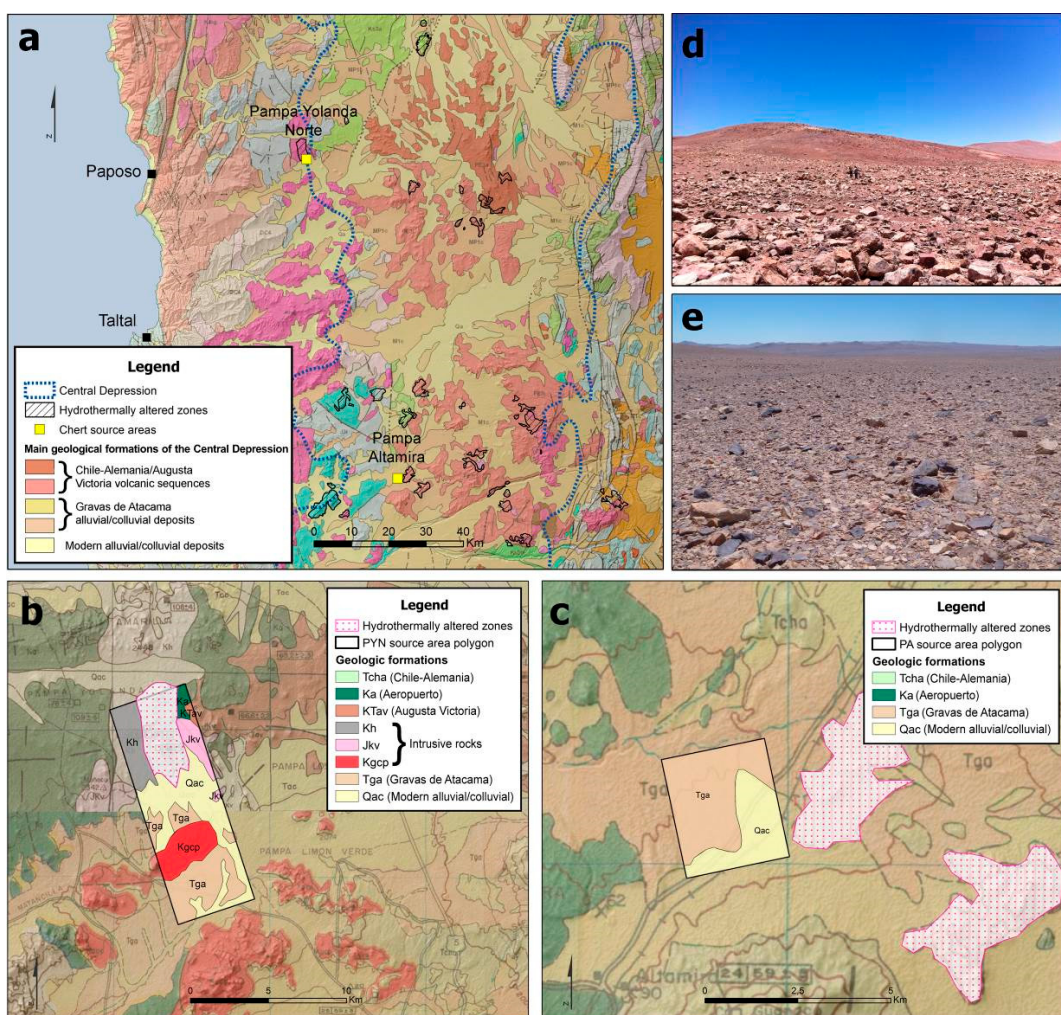


**Figure 2.** (a) Map of the study area showing the main geological formations within the Central Depression (dashed blue lines), hydrothermally-altered zones (black hatched polygons), and chert source areas (yellow squares), data from 1:1,000,000 geological map [82]; (b) and (c) source area of Pampa Yolanda Norte (b) and Pampa Altamira (c), showing associated geological formations and hydrothermally-altered zones (pink dotted polygons), data from 1:250,000 geological maps [80,81]; (d) and (e) panoramic views of Pampa Yolanda Norte and Pampa Altamira, respectively.

Chert source areas occur in the Central Depression as outcrops in hydrothermal alteration zones predominantly associated with the Chile-Alemania Formation, but also as secondary geological deposits in the overlying Gravas de Atacama Formation (Oligocene-Miocene) and in modern (Pleistocene/Holocene) alluvium and colluvium deposits [80,81]. The detritus flows of the latter formations fill low reliefs covering large areas in the Central Valley, where chert nodules carried from different outcrops abound [53,54].

The very low deposition rates documented in the area for the last 10 ka [55,56,69] and the very limited erosion processes during post-Pliocene times [83,84] define a mostly stable landscape in which primary and secondary deposits of chert, as well as evidence of their prehistoric exploitation, are exceptionally well-preserved in old and continuously exposed surfaces (the erosion and incision processes related to rain episodes during post-Pliocene humid phases have been limited to fluvial and alluvial features of a small scale [56,58,83]). Thus, the major geomorphological features between the foothills of the Andes and the coastal range, and the archaeological evidence located on them, have remained mostly unchanged [58,64,84]). This offers a perfect setting for the archaeological research of ancient lithic procurement systems through distributional large-scale approaches.

## 5. Materials and Methods

The methodological strategy proposed by this study integrates techniques from archaeology, geography, and geology. In order to reach its full potential, this approach requires the implementation of a series of linked work stages and specialized analysis techniques. In the following sections, the stages executed to date are presented sequentially, while those that are still in progress will be considered in the Discussion and Conclusions sections.

### 5.1. Construction of a Georeferenced Database

As an initial step, a baseline georeferenced database was constructed in QGIS®. This database included cartographic baseline data at a 1:50,000 scale, acquired from the Military Geographic Institute of Chile (IGM), and freely accessible hydrology, ecology, and topography (ASTER GDEM) geospatial data. The geological maps available for the area at a 1:250,000 scale [80,81] were also digitized and georeferenced in this GIS database.

Using online search tools from the Chilean Environmental Assessment Service (SEA) website, the existing CRM reports containing archaeological data for the interior desert (the area between the coastal range cliffs and the Andean foothills) were identified. The information they contained regarding prehistoric sites and finds was organized and standardized using a tabular database including the following data fields:

- UTM coordinates (WGS84 datum)
- site category
- horizontal extension (area)
- type and number of lithic artefacts recorded
- type of lithic raw materials recorded

This database also included the archaeological findings made by the research team in preliminary inspections of the area (see Figure 3 in Section 6.1. Details of the different datasets used in this research are presented in Supplementary Table S1).

### 5.2. Satellite Image Analysis

The second stage involved the acquisition, pre-processing, and study of Landsat 8 multispectral satellite images using QGIS. Four scenes were needed to cover the study area. These scenes were downloaded with minimum cloud cover (less than 3%) and pre-processed using the Semi-Automatic Classification Plugin (SCP, version 6) in QGIS. The pre-processing operations included atmospheric correction, application of the DOS1 method to the blue and green bands, and conversion to surface

reflectance values of the six spectral bands (bands 2 to 7) of the Landsat 8 OLI sensor, corresponding to a spectral range between the VIS and SWIR (0.45 and 2.35  $\mu\text{m}$ ).

After pre-processing, the Landsat scenes were assembled in a mosaic, from which a polygon of 22,500  $\text{km}^2$  (ca. 150  $\times$  150 km) of the study area was extracted as a subset. This subset, with a 30 m spatial resolution and six spectral bands, constituted the base dataset on which the subsequent analyses were conducted by applying basic image enhancement techniques for their visual interpretation.

False-color RGB composites were generated using different band combinations to highlight geological features. This first approach sought to produce a color image with optimal conditions for geological interpretation at a regional scale, by testing various combinations of Landsat SWIR, NIR, and VIS bands, which included RGB composites suggested by other studies to highlight geological features in arid and semi-arid environments [7,85,86].

Band-ratioing techniques were used to suppress variations in the reflectance of the scenes due to topography and grain-size variations, emphasizing differences in the spectral reflectance curves which favor the discrimination of mineral clusters that cannot be seen clearly in single-band examination [6,8,87,88]. Different Landsat band ratios recognized for their utility in mapping hydrothermal alteration zones [7,9,85,86] were tested in RGB false-color composites to enhance the visual discrimination of chert primary and secondary deposits associated with this kind of alteration zone. Finally, a third processed image was obtained from a PCA, with the aim of (1) reducing the redundant spectral data contained in the different Landsat bands to a limited set of new uncorrelated principal components (or PCs) [89] and (2) enhancing the subtle spectral information of new principal component images related to characteristics of lithic raw material that may not be noticeable in original bands' composition. The eigenvalues and eigenvector matrix of the PCA were examined and, together with the generated PCs, various RGB combinations of principal components were tested to identify potential chert-bearing geological formations.

### 5.3. Archaeological Fieldwork

Integration of the data from the two previous stages allowed us to (a) identify certain trends in the spatial organization of the archaeological record and the geology of the area, and (b) define spatially restricted zones of interest for targeted pedestrian surveys. To facilitate the detailed study of these zones, two polygons of 1  $\times$  30 km were selected as sampling zones and placed in order to cover two segments (the Western and Central Segments), which the baseline data signalled as relevant for the lithic provisioning dynamics within the study area [53,54]. Both segments make up an almost continuous altitudinal transect (with a gap of 10 km) covering the interior desert from 12 to 82 km east of the coastline and rising from 930 meters above sea level, in the lower reaches of the Cascabeles ravine, up to 2,275 meters above sea level in Pampa Flor de Chile, in the middle portion of the Central Depression (see Figure 7 in Section 6.3).

This strategy sought to generate a cross-sectional view of the coastal lithic supply systems deployed in the hyper-arid lands which extend between the coastal range and the western slopes of the Cordillera de Domeyko. For this purpose, the Western Segment of the survey transect was located in one of the main natural routes connecting the coastal platform with the Central Depression. In turn, the Central Segment was placed in the core area of the Central Valley, an area highlighted by preliminary studies as having a greater presence of actual and potential chert source areas [53,54]. The design of these segments avoided crossing areas heavily intervened by historic nitrate extraction operations and excluded, as far as possible, areas which had already been subject to archaeological survey by CRM projects.

The two survey polygons were traversed by parallel transects of west-east orientation, regularly spaced at 100 m intervals (the distance of 100 m between transects responds to a compromise between survey intensity and spatial coverage. This methodological decision considered the excellent archaeological visibility of the interior desert, which is favored by the complete absence of vegetation cover and the predominance of flat terrain.). The archaeological finds along these transects were

positioned with handheld GPS devices and their main features recorded as field notes and by digital photography. Additionally, specific archaeological studies were conducted in a targeted manner in discrete areas outside of the survey segments, areas that had been signalled by the baseline data previously collected as potential chert sources.

#### 5.4. GIS Integration

This last stage involved updating the GIS database with the new archaeological field data provided by the systematic pedestrian surveys. When integrated with the baseline information gathered from the available sources and generated by satellite remote sensing techniques, this detailed field data facilitated the assessment of the results of the remote sensing approach, in terms of both the geological (discrimination of types of chert) and geographical (size and location of the sources identified) resolution. All in all, this helped to gain a more thorough vision of the Southern Atacama lithic landscape.

The capabilities of GIS for data integration were exploited in this stage specifically as a means for assessing the accuracy of the remote sensing results by confronting them with the data provided by the conventional 1:250,000 geological maps, in addition to the archaeological field data contained in the “grey literature” and gathered during the aforementioned field studies.

Managing multiple information sources collected at different spatial resolutions is an unavoidable task in the reconstruction of ancient lithic landscapes [18], and GIS have greatly assisted this process in archaeological studies that range from local [90–92] and regional [18,93] to macro-regional scales [94].

## 6. Results

### 6.1. From the “Grey Literature” to the GIS Database

The review of the SEA database found 15 reports containing data of prehistoric archaeological findings within the interior desert. These findings were identified through systematic surveys in various patches of land comprising an area of ca. 390 km<sup>2</sup> [54]. The 1,193 records obtained from these sources were complemented by 37 new archaeological sites detected during preliminary inspection of the main ravines that dissect the Central Depression and the coastal range.

These 1,230 points of archaeological interest were systematized and integrated into the GIS geo-referenced database. All of them consist of locations with surface lithic scatters, only occasionally (3.3% of the records) associated with the remains of circular stone structures of very low architectural investment. The lithic categories reported in these locations are nodules, cores, hammerstones, flakes, and debris. Macroscopically diverse chert varieties, described as flint, chalcedonies, jaspers, and quartz, are the dominant raw materials (97.8% of records). Non-siliceous and coarse-grained silicified raw materials (quartzite, andesite, basalt, and tuff) are markedly less represented, occurring at a low frequency in assemblages with chert (in only 12 locations) and in 24 locations exclusively (2.2% of records) (Figure 3).

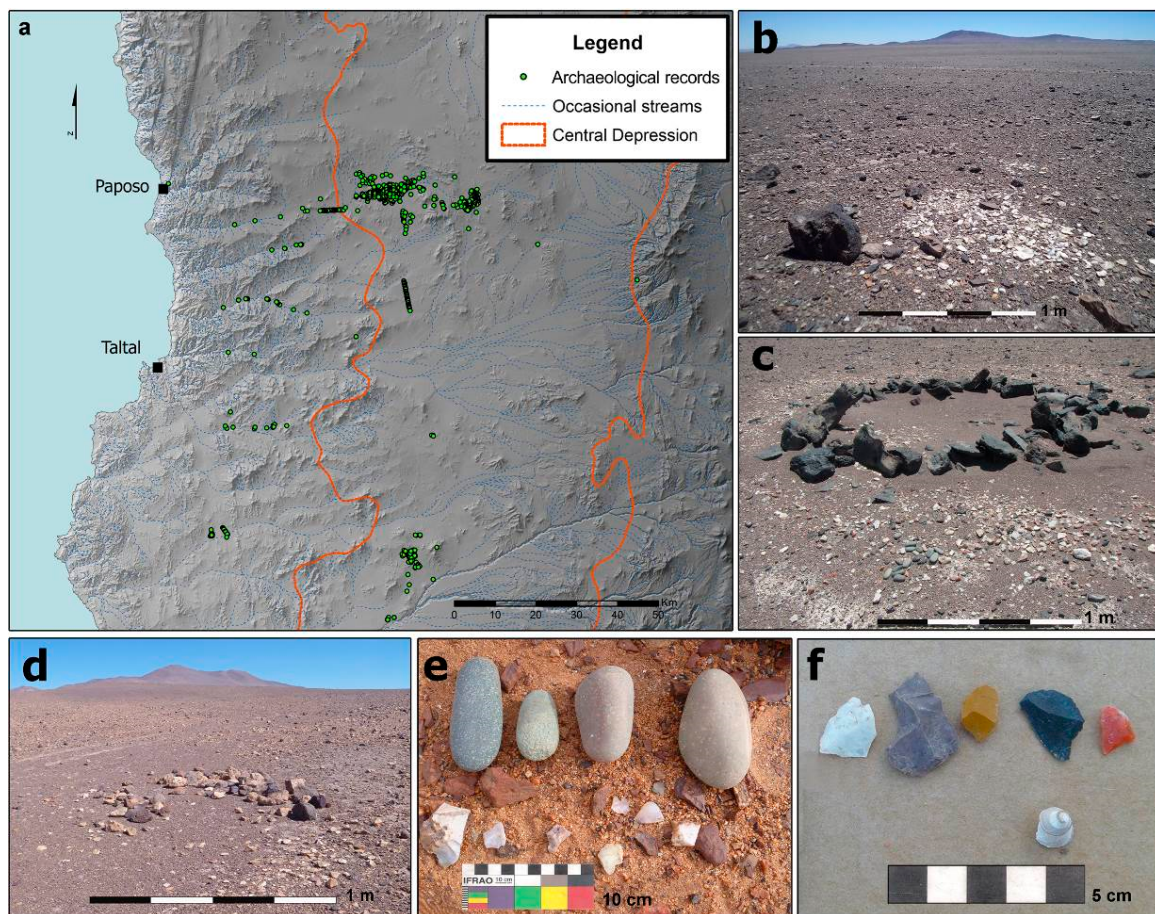


**Figure 3.** DEM of the study area showing the points of archaeological interest of the interior desert (green dots), the limits of the Central Depression (orange lines), and occasional streams (blue lines); (b) to (f) material assemblages of ephemeral prehistoric occupations in the core of the Atacama Desert.

The baseline data recovered from the “grey literature” and our initial inspections of the area allowed us to obtain an overview of the archaeological record of the interior desert. These georeferenced data, when incorporated into the GIS database with other thematic layers, provided key information for evaluating the potential of satellite remote sensing techniques, as will be described below. GIS integration of the results of these different lines of work was crucial for the planning of systematic fieldwork focused on specific areas of interest, the main results of which are presented in Section 6.3.

## 6.2. Satellite Remote Sensing the Lithic Landscape

In this subsection, the main results of the spectral analysis techniques applied to Landsat 8 multispectral imagery are summarized. More details about this preliminary analysis, including the use of complementary techniques of digital interpretation (material mapping and supervised classification), can be consulted in [53].

### 6.2.1. Band Combinations

Different band combinations were tested with the pre-processed Landsat 8 image of the study area, with the false-color composite of 7-6-2 (RGB) providing a greater visual contrast of the actual and potential chert-bearing geological formations. These formations are highlighted in light green, showing spatial correspondence with hydrothermal alteration zones registered in the geological 1: 250,000 charts [80,81], as well as with the two source areas of this raw material detected in preliminary field inspections (Pampa Yolanda Norte and Pampa Altamira). Meanwhile, the surrounding environment

is dominated by two other shades: blue, mainly in the area of mountains and plains of the Central Depression, and yellow, which generally coincide with the mountain ranges of both the coastal range in the west and the Cordillera de Domeyko in the east (Figure 4).

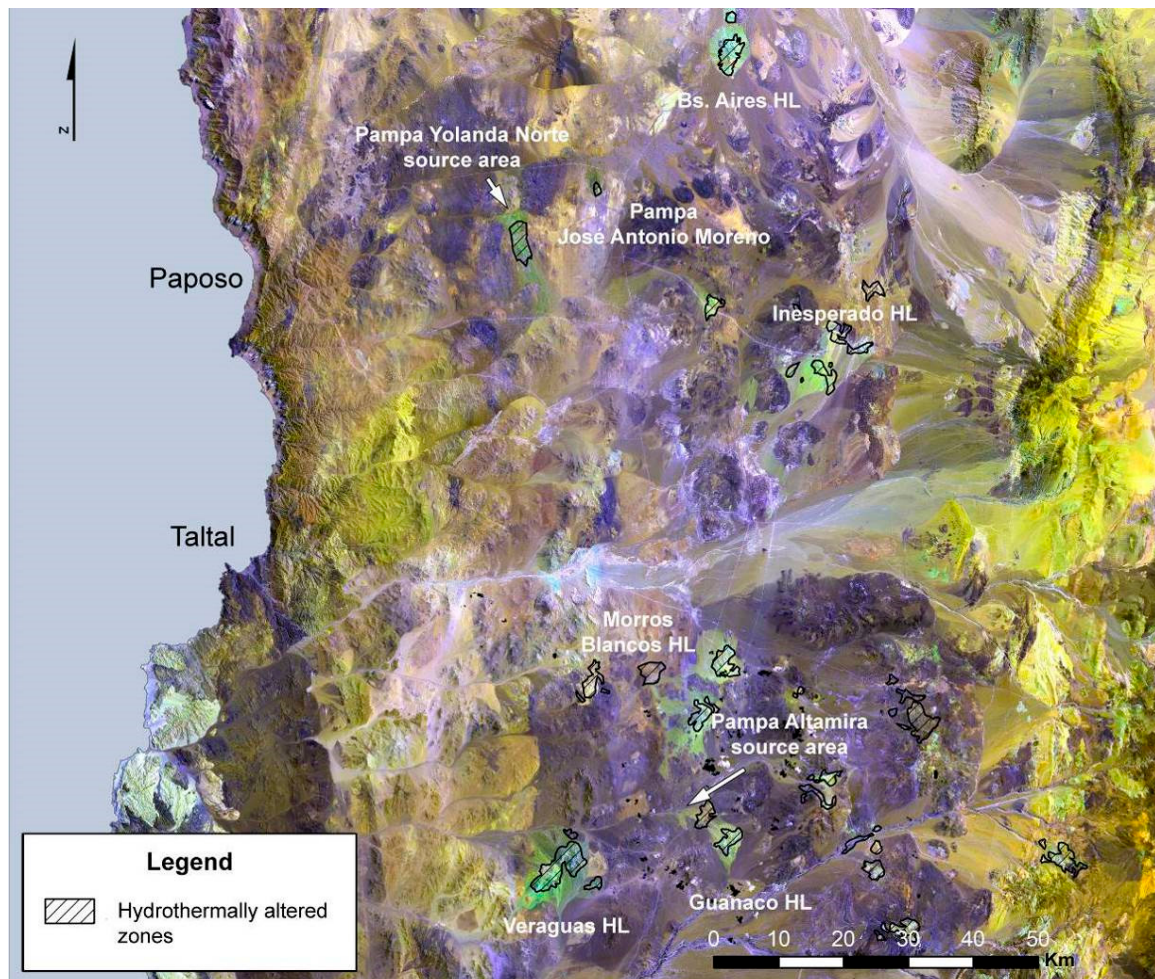


**Figure 4.** Landsat 8, bands 7-6-2 (RGB) false-color composite. Potential and actual chert source areas are highlighted in light green, and hydrothermally-altered zones are shown as black hatched polygons.

This first composite allowed us to observe a pattern of grouping of potential chert-bearing lithological units within the Central Depression, which broadly coincide with the location of the main hydrothermal alteration zones mapped on the geological charts. In the northern section of the Central Depression, the somewhat dispersed group formed by Cerro Punta Amarilla (Pampa Yolanda Norte), Pampa José Antonio Moreno, and the Inesperado and Buenos Aires hills stands out. In the southern section, the Veraguas, Guanaco, and Morros Blancos hills, together with Pampa Altamira, form a more compact grouping of extensive areas with the possible presence of chert-bearing deposits, together with other minor hydrothermal alteration zones towards the east.

#### 6.2.2. Band Ratios

Band ratios reported as informative in identifying hydrothermal alteration zones with Landsat scenes [6,7,9,85,86] were calculated and manipulated in the RGB guns of QGIS to determine the most appropriate combinations to effectively distinguish the lithological units of interest. The composite of ratios that best highlighted the spectral features of the different soil covers of the study area was  $R = 4/2$ ,  $G = 6/7$ ,  $B = 5$  [9,86] (Figure 5).

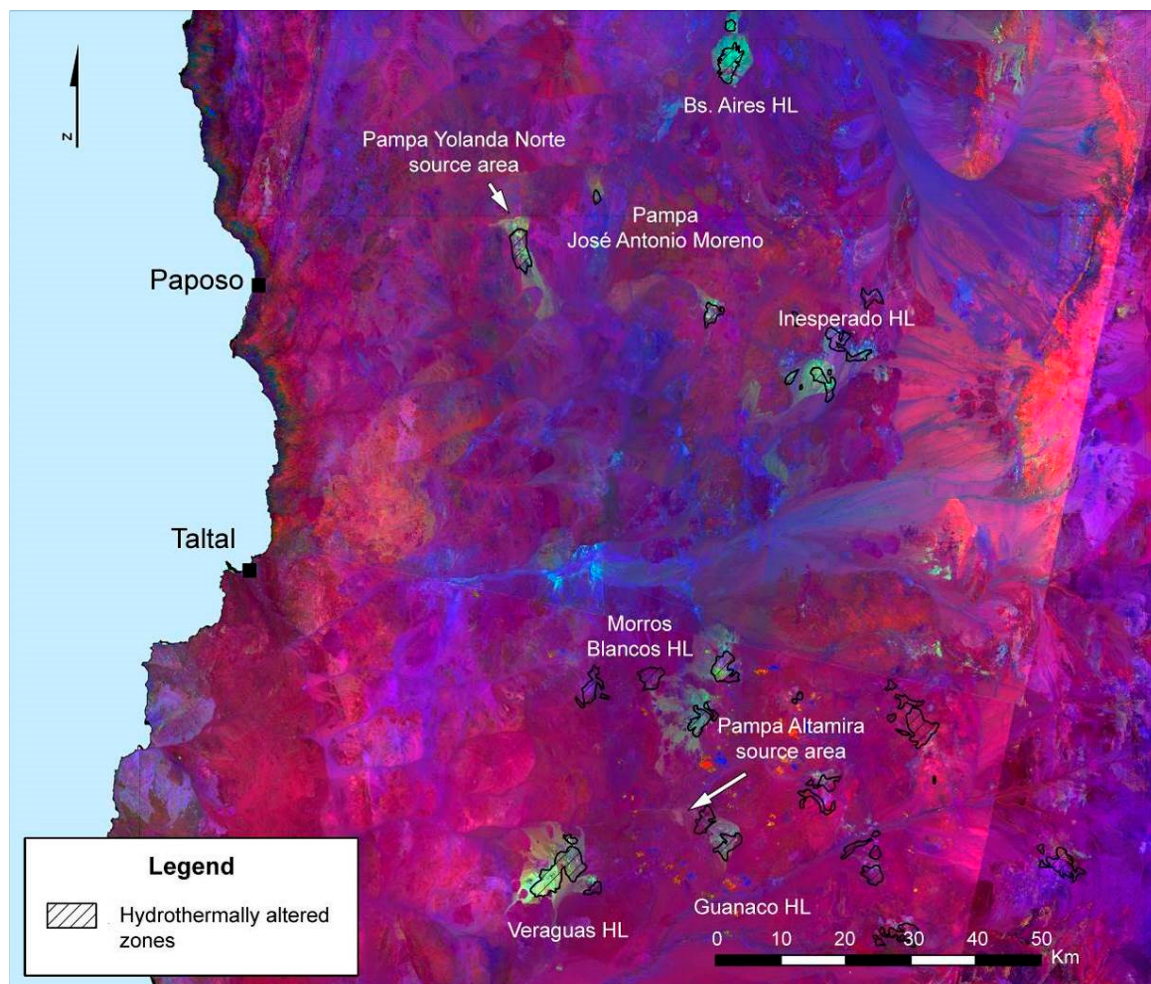


**Figure 5.** Landsat 8, band ratio 4/2-6/7-5 (RGB) false-color composite. Potential and actual chert source areas are highlighted in light green, and hydrothermally-altered zones are shown as black hatched polygons.

The band ratios generated improved the results obtained with band combinations. By accentuating differences of reflectance indicative of certain mineral groupings, the main geological formations of the Central Depression and the chert deposits that occur in this specific sector of Southern Atacama stand out. Ratio 4/2 (red) foregrounds continental volcanic sequences, which in the case of the Central Depression, are mainly represented by the Chile-Alemania Formation. Band 5 (blue) targets the calcareous and saline soils that form part of modern alluvial and colluvial deposits. The older alluvial/colluvial deposits of the Gravas de Atacama Formation appear in magenta, as they are mainly composed of detritus flows which carry clasts from the underlying Chile-Alemania Formation [80] and are mixed, when reaching lower grounds, with modern alluvial/colluvial deposits. Finally, ratio 6/7 highlights potential and actual chert-bearing deposits, which are clearly contrasted in a light green color against the predominantly magenta and blue background (further details under Section 7. Discussion).

#### 6.2.3. PCA

The third, and final, processed image was obtained from a PCA. PC 1 comprises 99.99% of the variance, which suggests that most of the variability in the Landsat scene is common to all the bands. The other subsequent components, although they represent only the remaining 0.00006% of variance in the data, enhance subtle spectral features of the original scene, which are useful for the mapping of

chert-bearing formations. The selection of PCs was made by examining the eigenvector matrix (Table 1), which showed contrasting relations between original bands and PCs. In this case, the combination of PC 5, 4, and 2 in the RGB guns turned out to be the most suitable for differentiating the lithological units of interest, contrasting strongly in intense magenta the actual and potential chert source areas on a background dominated by green and light green tones (Figure 6).

**Table 1.** Eigenvector matrix of Landsat 8 VNIR bands PCA.

Eigenvector/PC	PC 1	PC 2	PC 3	PC 4	PC 5	PC 6
Eigenvector 1	0.170988	-0.451865	-0.62058	0.0738699	0.521468	0.322607
Eigenvector 2	0.277532	-0.446888	-0.314157	-0.111879	-0.43326	-0.651415
Eigenvector 3	0.374354	-0.396037	0.301608	-0.0688847	-0.478003	0.61548
Eigenvector 4	0.44429	-0.246103	0.60082	0.115229	0.526232	-0.301425
Eigenvector 5	0.574989	0.480726	-0.166831	-0.63249	0.0927344	0.0425876
Eigenvector 6	0.474966	0.384187	-0.190792	0.750972	-0.162328	0.00979504

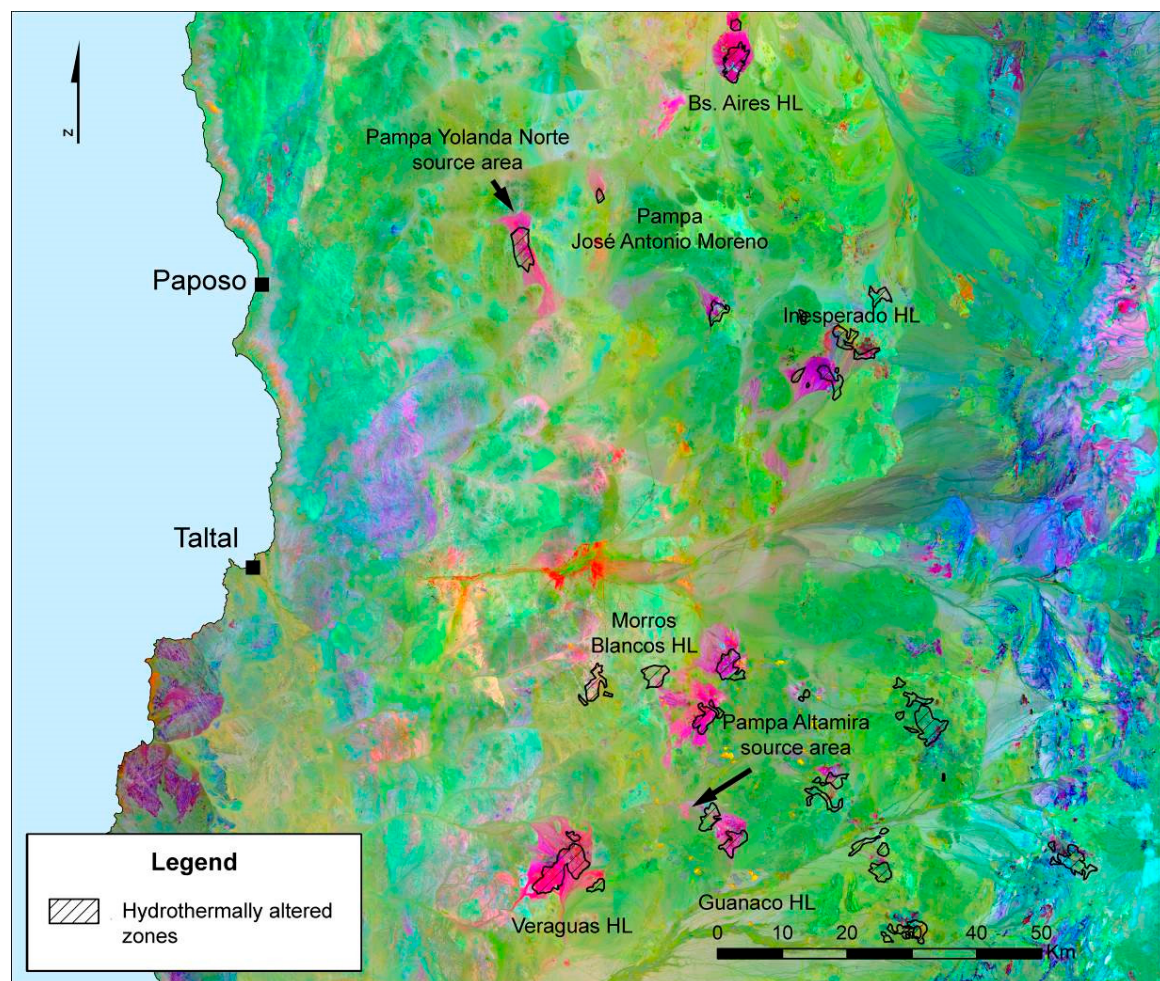


**Figure 6.** Landsat 8, PCs 5-4-2 (RGB) false-color composite. Potential and actual chert source areas are highlighted in magenta, and hydrothermally-altered zones are shown as black hatched polygons.

The PCA image yielded information which conforms with the band combination and band ratio RGB composites, in terms of the location of potential chert-bearing geological formations within the study area, a fact that is consistent with the archaeological and geological baseline data.

The integrated results of all these spectral analyses and the fieldwork detailed below, will be addressed in the Discussion section.

### 6.3. Stepping Inside the Core of the Atacama Desert

The pedestrian surveys covered 77 km<sup>2</sup> (39 km<sup>2</sup> in the Western Segment and 38 km<sup>2</sup> in the Central Segment) and resulted in the identification of a total of 1,517 points of archaeological interest. These correspond to locations with superficial lithic scatters, ranging from bounded and small low-density loci to large and diffuse areas composed of several lithic foci with a variable density. The lithic assemblages of these contexts reflect different stages of the reduction sequence of macroscopically diverse types of chert, the dominant raw material in 97.5% of the cases, and the only material documented in 85.5% of the cases. In turn, non-siliceous and coarse-grained silicified rocks (andesite, basalt, ignimbrite, sandstone, quartz, rhyolite, and tuff) comprise the only raw material in only 2.6% of the points.

In the Central Segment, with very few exceptions, only evidence of the primary processing of chert nodules was identified, including the production of bifacial cores and matrices (2.6% of the records). The intermediate and advanced stages of these raw material reduction sequences were predominantly documented in the Western Segment. This is consistent with the presence in the Central Segment of chert source areas and with the availability of a natural corridor (the Cascabeles and Portezuelo ravines) in the Western Segment, through which the reduction of chert pieces from the Central Depression sources to the coastal base and task camps took place (Figure 7).

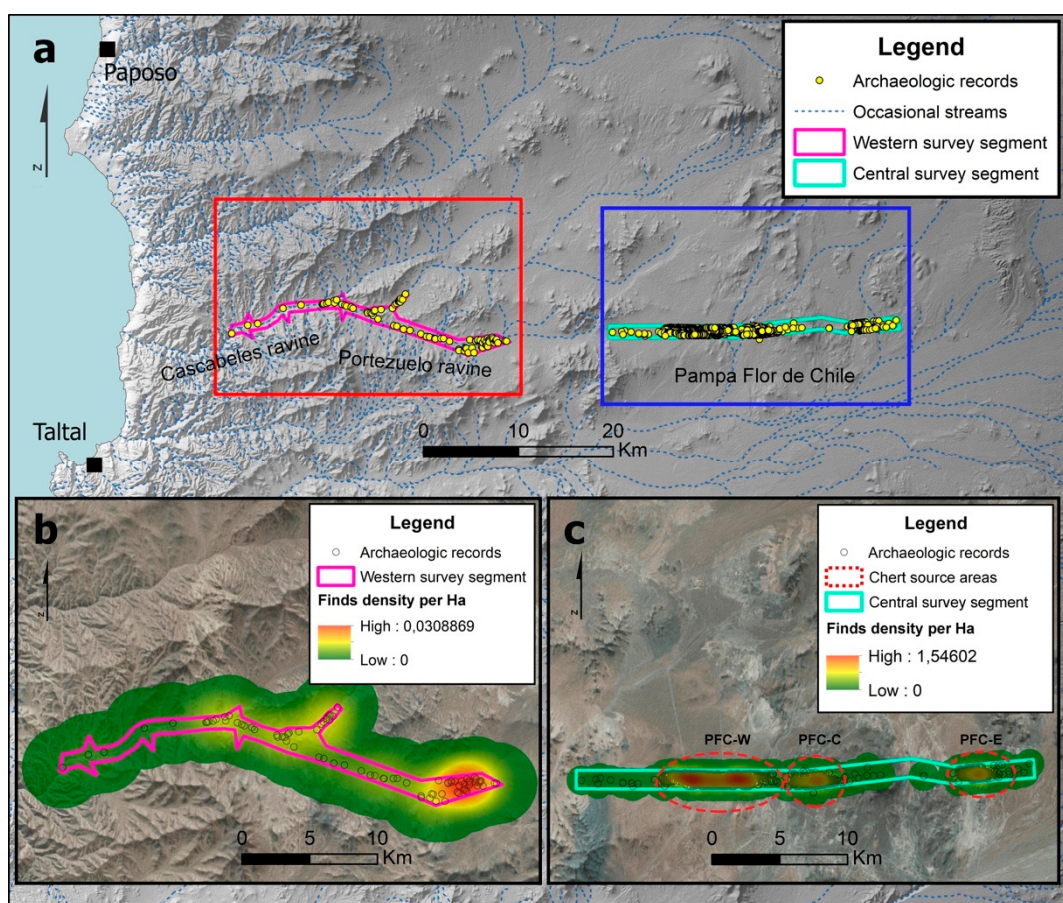


**Figure 7.** DEM of the study area showing the occasional streams (blue lines) and the locations with lithic scatters (yellow dots) recorded in the Western Segment (pink polygon) and Central Segment (light blue polygon) during systematic pedestrian surveys in the interior desert. Red box in (a) corresponds to a natural color composite (b) showing the Western Segment (pink polygon) and the archaeological finds (black circles) with their density per hectare. Blue box in (a) corresponds to a natural color composite (c) showing the Central Segment (light blue polygon); the archaeological finds (black circles) with their density per hectare; and the chert source areas Pampa Flor de Chile West, Center, and East (red circles).

In Pampa Flor de Chile (Central Segment), three new chert source areas were identified, which were named Pampa Flor de Chile West, Center, and East (PFC-W, PFC-C, and PFC-E). In the Western Segment, no source areas of this raw material were recorded, only low-density scatters of macrocrystalline quartz at the headwaters of the Portezuelo ravine.

The three chert sources in Pampa Flor de Chile can be added to those previously recorded in Pampa Yolanda Norte (PYN) and Pampa Altamira (PA), and to another chert source signalled by CRM reports and confirmed by the targeted field inspections (Arbiodo West or ARB-W), making a total of six main chert source areas. Focused archaeological and geological studies were conducted to characterize all these lithic sources and to collect “ground-truth” data for further studies, which are introduced as ongoing research lines in the following sections.

## 7. Discussion

The GIS integration of the data generated by the aforementioned analytical stages enabled us to obtain, with a low level of investment in terms of time and resources, an overview of the lithic landscape of this inland and little-studied portion of Southern Atacama. Although this is a preliminary and still coarse-grained approach, it has allowed us to corroborate certain aspects of interest, referred to in previous archaeological and geological studies, and to design strategies for systematic and focused fieldwork in a vast and harsh study area.

The different lines of evidence condensed in this investigation indicate that chert source areas are clearly clustered in the Central Depression, at linear distances between 40 and 80 km away from the modern coastline. None of these lithic procurement areas are found on the western flank of the study area (coastal platform and coastal range), with the exception of some of the deposits which comprise the large source of Pampa Yolanda Norte, a source located on the border between the coastal range and the Central Valley. On the eastern flank of the study area, which includes a portion of the western foothills of the Andes (Cordillera de Domeyko), chert only seems to be available in smaller and scattered deposits.

The absence of high-quality chert in the coastal platform and in the coastal range is consistent with the results of geological, petrographic, and geochemical studies, which report a predominance of intrusive rocks and, to a lesser extent, metasedimentary rocks in the coastal range between Taltal and Paposo [95]. This is a trend that characterizes the geology of this relief feature throughout the study area [80,81].

In the Andean foothills, as in the coastal range, hydrothermally-altered zones are scarce and widely scattered [80]. This is in line with the results of the remote sensing techniques deployed in this study, which show only faint traces of potential chert-bearing formations in both areas.

The spatial organization referred to above for the chert source areas is coherent with the archaeological record available for different sectors of the Southern Atacama, which points to a concentration in the Central Depression of the deposits of siliceous rocks accessed by local hunter-gatherer-fisher groups [46,48,50,53]. It has been suggested that this spatial configuration of the Southern Atacama lithic landscape was part of a broader regional pattern, within which the siliceous deposits, located at an average distance of 80 km from the coast, form an extensive system of approximately 800 km throughout northern Chile’s Central Valley [48]. Techno-functional and lithic reduction sequence analyses carried out in both coastal and interior prehistoric contexts support this idea, by signaling the presence of primary exploitations of chert nodules in the Central Depression and a marked predominance of small-sized flakes, mostly with no cortex, in the coastal assemblages [46–48,50,52,96].

Chert source areas in the Central Depression of the study area comprise primary and, especially, secondary, geological deposits. The outcrops are found, in most cases, in direct spatial association with (or close proximity to) hydrothermal alteration zones, mapped in the geological charts as part of the volcanic sequences of the Chile-Alemania Formation [80,81]. Nodules from these outcrops are carried by alluvial/colluvial deposits to distances of up to 15 km. [53,54]. It is in these large detritus

flows that locations of chert primary exploitation are most commonly recorded across the Southern Atacama [46,52–54].

The analysis of the multispectral Landsat images provides a significant advantage over the conventional 1:250,000 geological charts [80,81]: they do not only allow the main areas of hydrothermal alteration within the study area to be clearly highlighted, but they also bring about the possibility of distinguishing smaller areas with either primary or secondary deposits of this lithic raw material. This point will be demonstrated with three examples that compare the geological and geographical resolution of the 1:250,000 geological charts with the one obtained by remote sensing techniques. When available, the location of archaeological finds documented in CRM reports and by the preliminary inspections and systematic surveys conducted as part of this study, are included to show the aforementioned spatial relation of prehistoric lithic processing contexts and the chert deposits detected.

The first case (previously unknown primary deposits of chert) is illustrated by the Pampa Altamira source area, a single and relatively discrete primary outcrop (ca.  $2.7 \times 1.5$  km), the nuclear area of which covers lands assigned in the geological charts to the Gravas de Atacama Formation [82]. This deposit, despite being located not far from a hydrothermal alteration zone mapped in the geological charts, is not identified as such. Band combination 7-6-2, as well as the band ratio composite and PCA image, are able to clearly show it as a chert-bearing lithological deposit (Figure 8a,b).

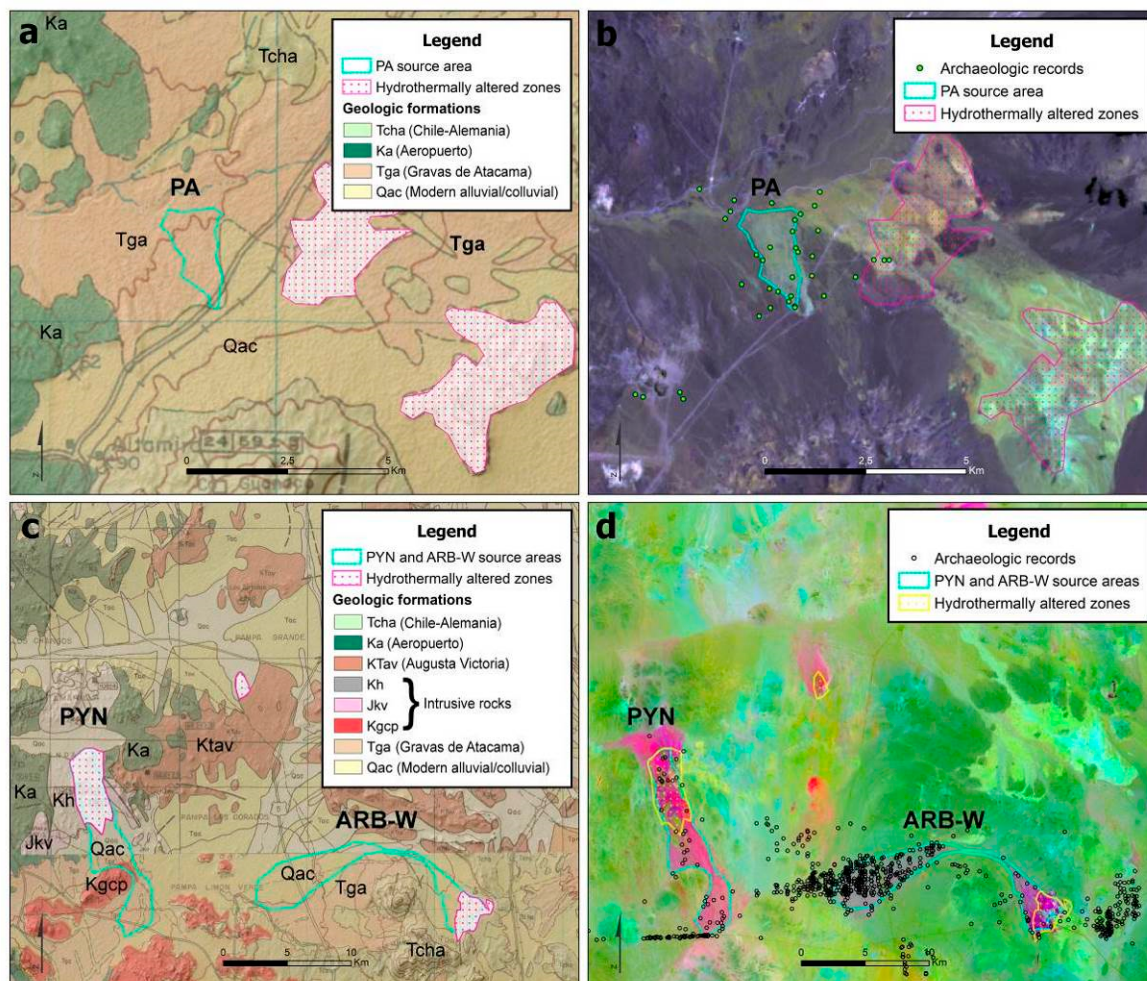


**Figure 8.** Comparison of 1:250,000 geological maps (a,c) [80,81] and processed satellite images: (b) 7-6-2 (RGB), and (d) PCs 5-4-2 (RGB), showing the geographical setting of chert source areas: (a,b) Pampa Altamira; (c,d) Pampa Yolanda Norte and Arbiodo West.

A good example of the second case (previously unknown secondary deposits of chert) can be found in the sources of Pampa Yolanda Norte and Arbiodo West, whose extensive secondary deposits are included in the geological charts as part of modern alluvial/colluvial deposits [80,81]. The spectral analysis of the Landsat scenes made it possible to detect both the primary and secondary deposits of these source areas, with Pampa Yolanda Norte standing out with a higher contrast (Figure 8c,d).

Another example worth mentioning is that of the Pampa Flor Chile East source areas, included in the geological charts within the Oligocene-Miocene detrital flows which constitute the Gravas de Atacama Formation [80]. The association of this chert-bearing secondary deposit to its primary source is not as direct, nor as clear, as in the previous cases. However, the analysis of the satellite images allows us not only to identify it as a secondary chert deposit, but also to infer a possible connection with the hydrothermal alteration zones registered 10 km to the northeast, in Cerro Inesperado (Figure 9a,b).

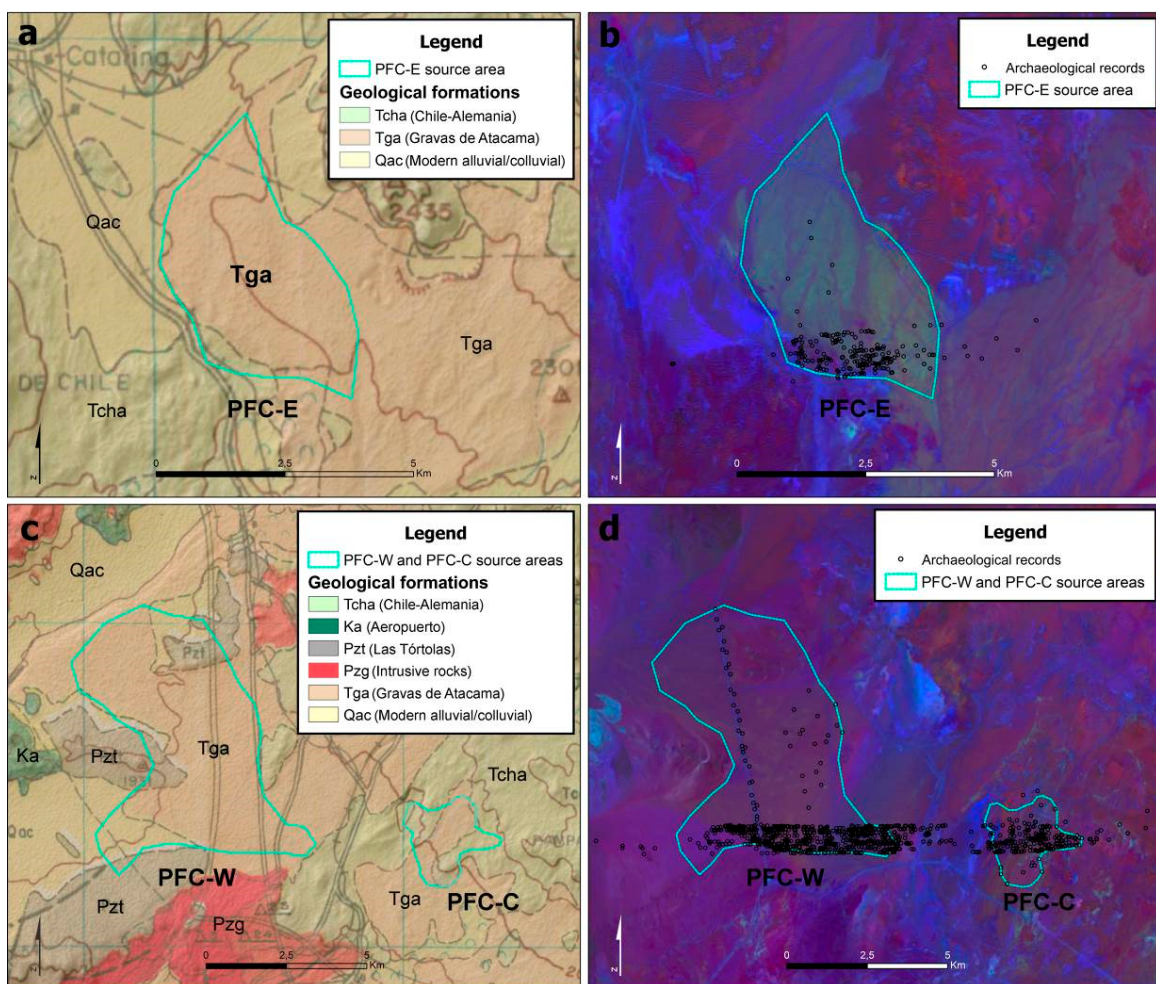


**Figure 9.** Comparison of 1:250,000 geological map (a,c) [80] and band ratio 4/2-6/7-5 (RGB) false-color composite (c,d), showing the geographical setting of chert source areas: (a,b) Pampa Flor de Chile East; (c,d) Pampa Flor de Chile West and Pampa Flor de Chile Centre.

Finally, the source areas of Pampa Flor de Chile West and Pampa Flor de Chile Centre present a more complex scenario for the interpretation of the processed satellite images. The spectral analysis only shows a very subtle sign of altered rocks in the secondary deposits of Pampa Flor de Chile West, assigned in the geological charts to the Gravas de Atacama Formation [80]. Meanwhile, in the area where the small outcrops of Pampa Flor de Chile Center are located, only traces of possible hydrothermal alteration zones are detected, which extend over land assigned to the Chile-Alemania and Gravas de Atacama formations. The low performance of remote sensing techniques to clearly map

these source areas may have to do with the brief lateral extension of the Pampa Flor de Chile Centre outcrops (averaging less than  $0.5 \times 0.3$  km) and their location on the boundary of two geological formations. Furthermore, Pampa Flor de Chile West chert deposits are presumed to be residual, meaning that the bedrock that originally housed them has been completely eroded [79]. This could explain the low spectral signal of these secondary deposits, which are thought to be relatively older and/or more heavily reworked than any others (Figure 9c,d).

The ability to map the chert carrier lithological units shown by the satellite remote sensing approach adopted in this study is derived from the presence of diagnostic spectral features of hydrous minerals in the VNIR range (0.3–2.5 um), which can be used as an indicator of hydrothermal alteration zones [5,6,9]. These hydrous minerals have high reflectance in the 1.55–1.75 um range and high absorption at 2.08–2.35 um, a fact that explains the sharp contrast achieved by using the SWIR Landsat bands 6 and 7 in the RGB band ratio composite 4/2-6/7-5 (Figure 10).

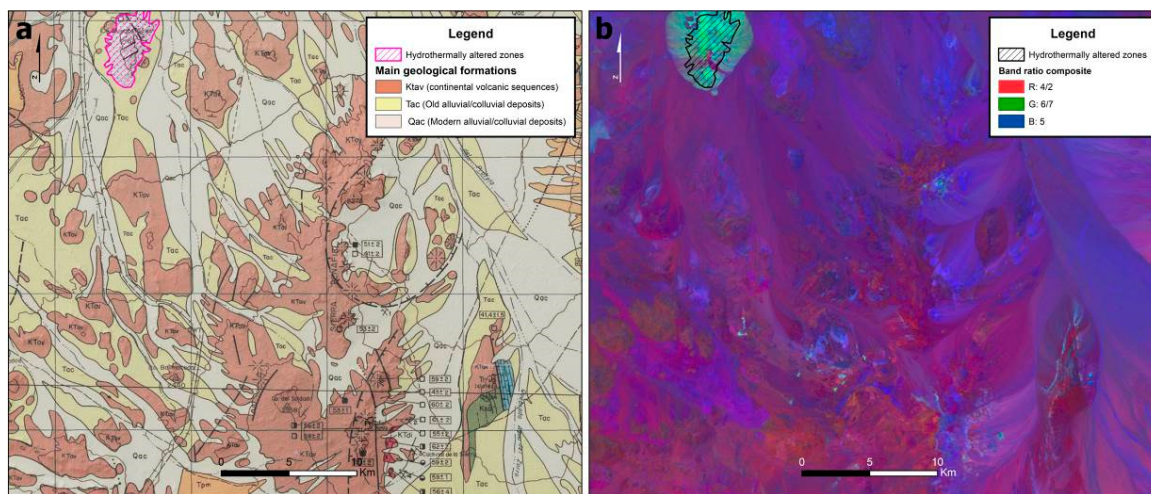


**Figure 10.** Comparison of: (a) 1:250,000 geologic map [83]; and (b) 4/2, 6/7, 5 Landsat 8 RGB band ratio composite for a section in the northeastern portion of the study area. The hydrothermally-altered zone (green area) corresponds to the Buenos Aires hill.

The near-infrared band 5 helped, in the absence of vegetation cover [97], to highlight the aforementioned contrast by showing the saline (nitrate-rich) and evaporitic soils, modern alluvial/colluvial deposits, and the more recently exposed calcareous soils of the hyper-arid Central Depression in blue. Meanwhile, the 4/2 ratio has the capacity to detect the presence of iron oxide-rich soils, which can be found in hydrothermal alteration zones [5,6,9], but which also have occurrences unrelated to them, such as in sedimentary red beds, volcanic rocks, and weathered alluvium [5].

The latter seems to be the case in our study area, where the 4/2 ratio highlights not only the hydrothermally-altered zones (due to the hydrothermal iron minerals), but also the iron oxide-rich volcanic sequences of the Central Depression (Chile-Alemania and Augusta Victoria Formations), which are shown in reddish shades in the band ratio composite. In correspondence to this, the magenta color in the processed image is presumed to be marking the erosive deposits that originated from those volcanic sequences, the mantling gravels of the Gravas de Atacama Formation, deposits that become progressively mixed with modern alluvial/colluvial detrital flows as they approach the flatlands of the Central Valley.

The inspection of the PCA eigenvector matrix supports the aforementioned results, since principal components 4 and 2, used in the PCA false color composite, account for differences between bands 6 and 7, and of these SWIR bands with bands 1 to 5, respectively (Table 1).

The capacity of Landsat VNIR bands to map prehistoric chert source areas is based on their ability to target alteration minerals which are spectrally active within this range due to the presence of water, carbonate, sulfate, and hydroxyl groups [6,9,58]. These alteration minerals can be found in the core

area of hydrothermally-altered zones, which are related to highly silicified chert outcrops in our study area. However, they can also be traced in the coarse-grained fraction represented by scattered lithic debris that remains on the surface surrounding ancient chert quarry areas [19]. Even in a low relative proportion, these freshly exposed rocks can provide a characteristic spectral signal which is useful for satellite remote sensing studies [19], making the mapping of extensive chert-bearing secondary deposits possible, as the results here presented show.

Although the visual and digital analysis of Landsat VNIR bands stands out as a great tool for the initial lithological mapping of a large and understudied area, its scope is limited to providing a broad-brush pattern of hydrothermal alteration, pointing out geological deposits of possible interest [7]. If a higher degree of geographical and geological resolution is desired, a combined use of VNIR and thermal (TIR) bands could provide a more detailed approach. This is suggested by recent studies using Landsat 8 TIR bands (10 and 11) along with VNIR bands to map alteration zones [98] and, especially, by research projects that take advantage of the SWIR and TIR bands of the ASTER sensor for this same purpose [99,100].

The greater number and narrower bandwidth of ASTER SWIR and TIR bands when compared to the ones captured by Landsat sensors offer the possibility of discriminating between minerals that are associated with phyllitic, argillic, and propylitic alteration zones in the SWIR range [100,101], and to target chert and other siliceous and silicified rock types according to variations in terms of their content of  $\text{SiO}_2$  and the crystal structure of silicate minerals, which are reflected in shifts in spectral features within the 7 to 14  $\mu\text{m}$  TIR range [7,102]. These capacities of ASTER images allow researchers to move from mapping alteration indices (with Landsat), to the generation of mineral indices, which can be used in the study of alteration zones, differentiating them by their associated mineral assemblages and alteration intensity [9].

The procurement, processing, transport, and use of chert in the Southern Atacama configured a vast and complex lithic landscape. Multiple source areas bearing diverse chert types with overlapping macroscopic features were exploited across large extensions of land and over long time spans. To cope with this challenging scenario, the mapping of the potential source areas of the widest possible range of chert types and the study of the differential distribution of these toolstone varieties in the lithic assemblages of local base and task camps are considered critical steps [18]. In order to address this, the accumulated variation within and between the chert types present in the archaeological and geological contexts of the study area must be examined [79,103–105].

Accordingly, this project's ongoing research includes the systematic recovery and VNIR and FTIR reflective spectroscopic analysis [23] of geological chert samples collected in the six chert sources currently known for the study area, and of chert artefacts (unmodified flakes) selected from two types of locations: on the one hand, lithic assemblages of five coastal settlements with stratigraphic deposits dated between 11,500 and 1,500 cal. BP; and, on the other hand, assemblages from surface lithic scatters of six processing locations recorded during pedestrian surveys conducted by the research team in the interior desert [53,54]. This approach will enable us not only to confidently source those archaeological artefacts which fall within the range of variation documented in the six source areas already located, but also to explore the use of the detailed spectral "ground truth" data provided by the VNIR and FTIR analysis of these prehistoric chert samples in the remote detection of new potential chert sources via the digital processing of ASTER L1B images.

To address the interpretation of the Southern Atacama interior desert's archaeological record diachronically is a complex task. The very low deposition rates of the area normally prevent the burial and preservation of organic materials that could be dated with traditional methods. Thus, lithic surface assemblages are the main, and usually the only, evidence from which archaeological inferences about the human occupational history of this landscape can be grounded. This fact, together with a static conception of the paleoenvironmental conditions of this part of the Atacama Desert, has reinforced a monolithic vision of the area as a geographical barrier and or a territory exclusively used for inter-zonal mobility and the provisioning of high-quality lithic resources [54].

In order to challenge the aforementioned vision, the different paleoenvironmental and social scenarios that could have promoted or restricted more stable and/or intense human occupation in the core of the Atacama Desert, must be evaluated [54,75,76].

Consequently, the aforementioned approach via VNIR and FTIR reflective spectroscopic analysis selected artefacts of macroscopically diverse chert types from archaic coastal basecamps for provenance studies, targeting radiocarbon-dated deposits that represent the six main periods in which the prehistoric chrono-cultural sequence of the area has been analytically divided [50].

The coastal chert artefacts' spectral data are currently subject to statistical analysis in order to assess if their origin corresponds to one of the six source areas under study. Complementarily, their spectral signature will inform targeted remote sensing techniques to locate previously unknown potential chert source areas.

On the other hand, technological and morpho-functional analysis of chert artefacts recovered from the interior desert lithic assemblages will provide valuable information in terms of lithic reduction sequences and transport strategies to assess technological strategies and site function. Spectroscopic analysis of these artefacts will yield "ground truth" data to establish hypothetical connections between the coastal contexts and the interior desert's chert source areas, connections that will be further explored by the generation of GIS mobility models.

To complement the abovementioned lines of evidence, the geological and archaeological data systematically collected in the chert source areas under study, in terms of abundance, distribution, quality, and size of the "packages" available [18,106], will be incorporated. This final integration will grant the assessment of shifts in lithic procurement strategies, such as differential access to the sources, exploitation intensity, raw material selectivity, core reduction, and blank and or tool production techniques, which can be correlated with changes in the settlement pattern, subsistence, and technological organization documented along the archaic sequence for the hunter-gatherer communities of the Southern Atacama coast [45,47,50].

Preliminary results indicate that the archaeological record of the interior desert, in general terms, conforms to the lithic provisioning models proposed for Atacama [46,48]. A vast dominance of primary chert processing contexts is recorded in the Central Depression, located to a great extent in spatial correspondence with chert-bearing alluvial/colluvial deposits. Moving towards the coast, progressively advanced stages of the reduction of this raw material are found in ephemeral sites located along the dry valleys of the area, relief features used as natural corridors by local prehistoric groups. Nevertheless, evidence of other kinds of activities has also been detected in the area, such as hunting and processing gear (unifacial and bifacial lithic instruments), coastal cobbles with red pigment, and rock art in small rock panels along the Portezuelo ravine [54,107].

Although recorded in small frequency, this other evidence is added to differences in terms of architectural investment (e.g. number of circular structures) and artefactual and ecofactual content of the sites (sea shells and fish bones from the Pacific Ocean, terrestrial faunal remains, and vegetal fibers from higher Andean floors), to configure a more diverse and dynamic prehistoric setting that needs to be discussed considering social and ecological processes at a regional scale.

## 8. Conclusions

The purpose of our case study was to illustrate the capacity of a GIS-based remote sensing approach to delimit, in an informed and effective manner, the areas of higher potential interest in the analysis of lithic provisioning systems in extensive and understudied desert landscapes.

The systematization of georeferenced archaeological data contained in the "grey literature" of CRM projects and its GIS integration with basic, and easily accessible, thematic layers, can make it possible to gain a panoramic view of the archaeological record of a study area. Complementary, basic techniques of image manipulation applied to freely accessible multispectral satellite scenes of a moderate spatial and spectral resolution can contribute towards a rapid acquisition of a general

knowledge of the area in terms of the distribution of geological formations potentially carrying lithic resources of interest.

The large swath width of the Landsat sensors offers the possibility to cover vast extensions of land by handling only a small number of scenes. This greatly facilitates pre-processing and mosaicking of Landsat VNIR bands, which can be done with user-friendly tools and plugins in open source software, such as QGIS. This same software allows for the visualization and analysis of multispectral images, easily integrating satellite remote sensing data in a georeferenced database with different thematic layers. The coarse-grain pattern of lithic resource availability that this GIS-based approach provides helps to target spatially restricted areas of interest for archaeological fieldwork and, also, informs about the type and number of additional satellite images with a higher spatial and or spectral resolution that could be purchased, if the mapping of geological deposits bearing more specific types of lithic raw materials is a desired goal.

This case study illustrates the usefulness of satellite remote sensing analysis of Landsat images to complement the information available in basic geological charts with data of a finer and more appropriate spatial resolution. This can be used for the mapping of lithic resources, such as chert, which were of great relevance in the technological organization of prehistoric hunter-gatherer populations in different parts of the world.

The research strategy deployed provides new data regarding the availability and distribution of high-quality primary and secondary chert deposits in a large portion of the Southern Atacama. Such data offers a solid basis when facing the complex task of reconstructing the archaic lithic landscape of the area.

Other lines of research are currently being developed in order to access higher levels of geological and geographical resolution in the survey of the regional structure of lithic resources, and to link the data obtained in the different chert source areas studied with the large bulk of archaeological evidence gathered for the interior desert and the arheic coast of the Atacama in this, and previous, research.

Provenance studies using VNIR and FTIR reflective spectroscopic analysis will make it possible to trace the source areas of chert artefacts from archaic coastal deposits and superficial hinterland contexts. More sophisticated remote sensing techniques, applied to the higher spectral resolution ASTER satellite images, will assist in refining the lithological mapping of the study area and tracking new potential chert sources. Furthermore, GIS models will be explored to model the main mobility basins through which archaic coastal settlements were connected with the chert source areas of the Central Depression. Finally, the processing of geological and archaeological data systematically recovered from the six source areas studied up to now, will enable a more thorough evaluation of the socio-ecological factors which may have influenced differential access to the chert sources of the Southern Atacama in prehistoric times.

To sum up, the reconstruction of the lithic landscape requires the innovative integration of analytical techniques developed by different disciplines. This integration is fundamental in establishing solid grounds for the archaeological study of the material patterns of human behavior, the traces of which are accumulated in locations widely scattered in space, but recurrently occupied during extensive chronological sequences. This scenario is not exclusive to our area of study, but is transversal to different environmental and cultural contexts, as it is an inherent dimension of lithic production systems. Their study on a landscape scale and over broad time spans is a necessary task, and the methodological strategy presented here has the potential to significantly facilitate this endeavor, both in the desert lands of northern Chile and in arid and semi-arid environments of other latitudes.

**Supplementary Materials:** The following are available online at <http://www.mdpi.com/2072-4292/11/7/869/s1>, Table S1: Basic information of the datasets used in this study.

**Author Contributions:** Conceptualization, C.B. and C.P.; methodology, C.B. and Y.K.; formal analysis, C.B.; investigation, D.S., C.F., C.B., L.O., and P.A.; writing—original draft preparation, C.B. and C.P.; writing—review and editing, C.B., C.P., Y.K., D.S., C.F., L.O., and P.A.; visualization, C.B.; supervision, C.B.; project administration, D.S.; funding acquisition, D.S., P.A., L.O., C.F., and C.B.

**Funding:** This research was funded by Proyecto Fondecyt 1151203 and Beca CONICYT-PCHA/Doctorado Nacional/2015-21150953.

**Acknowledgments:** Luca Sitzia for his geological assistance; the team members involved in field work carried out in the interior desert of Taltal: Ximena Power, Sonia Parra, Ignacio Monroy, Patricio Galarce, Luca Sitzia Carlos Uribe, Valentina Hernández, Catalina Aliste, and Gabriela Marcelo; and Lautaro Núñez for his valuable guidance.

**Conflicts of Interest:** The authors declare no conflicts of interest.

## References

1. Dimitrios, A.; Agapiou, A.; Diofantos, H.; Sarris, A. Remote Sensing Applications in Archaeological Research. In *Remote Sensing—Applications*; Escalante, B., Ed.; InTech: London, UK, 2012.
2. Comer, D.C.; Harrower, M.J. *Mapping Archaeological Landscapes from Space*; Springer: New York, NY, USA, 2013.
3. Forte, M.; Campana, S. (Eds.) *Digital Methods and Remote Sensing in Archaeology. Archaeology in the Age of Sensing*; Springer: New York, NY, USA, 2016.
4. Rowan, L.C.; Wetlaufer, P.H.; Goetz, A.F.H.; Billingsley, F.C.; Stewart, J.H. *Discrimination of Rock Types and Detection of Hydrothermally Altered Areas in South-Central Nevada by the Use of Computer-Enhanced ERTS Images*; U.S. Govt. Print. Off.: Washington, DC, USA, 1974.
5. Abrams, M.J.; Brown, D.; Lepley, L.; Sadowski, R. Remote sensing for porphyry copper deposits in southern Arizona. *Econ. Geol.* **1983**, *78*, 591–604. [[CrossRef](#)]
6. Sultan, M.; Arvidson, R.E.; Sturchio, N.C.; Guinness, E.A. Lithologic mapping in arid regions with Landsat thematic mapper data: Meatiq dome, Egypt. *GSA Bull.* **1987**, *99*, 748–762. [[CrossRef](#)]
7. Sabins, F. Remote sensing for mineral exploration. *Ore Geol. Rev.* **1999**, *14*, 157–183. [[CrossRef](#)]
8. Gad, S.; Kusky, T. Lithological mapping in the Eastern Desert of Egypt, the Barramiya area, using Landsat thematic mapper (TM). *J. Afr. Earth Sci.* **2006**, *44*, 196–202. [[CrossRef](#)]
9. Van der Meer, F.D.; van der Werff, H.M.A.; van Ruitenbeek, F.J.A.; Hecker, C.A.; Bakker, W.H.; Noomen, M.F.; van der Meijde, M.; Carranza, E.J.M.; Smeth, J.B.D.; Woldai, T. Multi- and hyperspectral geologic remote sensing: A review. *Int. J. Appl. Earth Obs. Geoinf.* **2012**, *14*, 112–128. [[CrossRef](#)]
10. Goodyear, A. *A Hypothesis for the Use of Cryptocrystalline Raw Materials Among Paleo-Indian Groups of North America*; Research Manuscript Series; 1979; Available online: [https://scholarcommons.sc.edu/cgi/viewcontent.cgi?referer=https://scholar.google.com.hk/&httpsredir=1&article=1126&context=archanth\\_books](https://scholarcommons.sc.edu/cgi/viewcontent.cgi?referer=https://scholar.google.com.hk/&httpsredir=1&article=1126&context=archanth_books). (accessed on 10 April 2019).
11. Gardner, W.M. Stop me if you've Heard This one Before: The Flint Run Complex Revisited. *Archaeol. East. N. Am.* **1983**, *11*, 49–64.
12. Gould, R.A.; Saggers, S. Lithic Procurement in Central Australia: A Closer Look at Binford's Idea of Embeddedness in Archaeology. *Am. Antiq.* **1985**, *50*, 117–136. [[CrossRef](#)]
13. Bamforth, D.B. Technological Efficiency and Tool Curation. *Am. Antiq.* **1986**, *51*, 38–50. [[CrossRef](#)]
14. Andrefsky, W. Raw-material availability and the organization of technology. *Am. Antiq.* **1994**, *59*, 21–34. [[CrossRef](#)]
15. Bailey, G. Concepts, time-scales and explanations in economic prehistory. In *Economic Archaeology: Towards an Integration of Ecological and Social Approaches*; Sheridan, A., Bailey, G., Eds.; British Archaeological Reports: Oxford, UK, 1981; pp. 97–117.
16. Foley, R. A Model of Regional Archaeological Structure. *Proc. Prehist. Soc.* **1981**, *47*, 1–17. [[CrossRef](#)]
17. Dunnell, R.; Dancey, W. The siteless survey: A Regional scale data collection strategy. *Adv. Archaeol. Method Theory* **1983**, *6*, 267–287.
18. Barrientos, G.; Catella, L.; Oliva, F. The Spatial Structure of Lithic Landscapes: The Late Holocene Record of East-Central Argentina as a Case Study. *J. Archaeol. Method Theory* **2015**, *22*, 1151–1192. [[CrossRef](#)]
19. Carr, T.; Turner, M. Investigating regional lithic procurement using multi-spectral imagery and geophysical exploration. *Turner* **1996**, *3*, 109–127. [[CrossRef](#)]
20. Rosendahl, S. Lithic Procurement Strategies in Early Prehistoric Cyprus: A Predictive Model. Master's Thesis, University of Leicester, Leicester, UK, 2010.

21. Deroin, J.-P.; Téreygeol, F.; Heckes, J. Evaluation of very high to medium resolution multispectral satellite imagery for geoarchaeology in arid regions—Case study from Jabali, Yemen. *J. Archaeol. Sci.* **2011**, *38*, 101–114. [[CrossRef](#)]
22. Vining, B. Reconstructions of local resource procurement networks at Cerro Baúl, Peru using multispectral ASTER satellite imagery and geospatial modeling. *J. Archaeol. Sci. Rep.* **2015**, *2*, 492–506. [[CrossRef](#)]
23. Parish, R.M. Reflectance Spectroscopy as a Chert Sourcing Method. *Archaeol. Pol.* **2016**, *54*, 115–128.
24. Thompson, V.D.; Arnold, P.J.; Pluckhahn, T.J.; Vanderwarker, A.M. Situating Remote Sensing in Anthropological Archaeology. *Archaeol. Prospect.* **2011**, *18*, 195–213. [[CrossRef](#)]
25. Banaszek, L.; Cowley, D.C.; Middleton, M. Towards National Archaeological Mapping. Assessing Source Data and Methodology—A Case Study from Scotland. *Geosciences* **2018**, *8*, 272. [[CrossRef](#)]
26. Agapiou, A.; Hadjimitsis, D.G.; Georgopoulos, A.; Sarris, A.; Alexakis, D.D. Towards an Archaeological Index: Identification of the Spectral Regions of Stress Vegetation due to Buried Archaeological Remains. In *Progress in Cultural Heritage Preservation*; Springer: Berlin/Heidelberg, Germany, 2012; pp. 129–138.
27. Cerra, D.; Agapiou, A.; Cavalli, R.M.; Sarris, A. An Objective Assessment of Hyperspectral Indicators for the Detection of Buried Archaeological Relics. *Remote Sens.* **2018**, *10*, 500. [[CrossRef](#)]
28. Fradley, M.; Sheldrick, N. Satellite imagery and heritage damage in Egypt: A response to Parcak et al. (2016). *Antiquity* **2017**, *91*, 784–792. [[CrossRef](#)]
29. Verhoeven, G. Are We There Yet? A Review and Assessment of Archaeological Passive Airborne Optical Imaging Approaches in the Light of Landscape Archaeology. *Geosciences* **2017**, *7*, 86. [[CrossRef](#)]
30. Harrower, M.; McCorriston, J.; Oches, E.A. Mapping the roots of agriculture in southern Arabia: The application of satellite remote sensing, global positioning system and geographic information system technologies. *Archaeol. Prospect.* **2002**, *9*, 35–42. [[CrossRef](#)]
31. Siart, C.; Eitel, B.; Panagiotopoulos, D. Investigation of past archaeological landscapes using remote sensing and GIS: A multi-method case study from Mount Ida, Crete. *J. Archaeol. Sci.* **2008**, *35*, 2918–2926. [[CrossRef](#)]
32. Salvi, M.C.; Salvini, R.; Cartocci, A.; Kozciak, S.; Gallotti, R.; Piperno, M. Multitemporal analysis for preservation of obsidian sources from Melka Kunture (Ethiopia): Integration of fieldwork activities, digital aerial photogrammetry and multispectral stereo-IKONOS II analysis. *J. Archaeol. Sci.* **2011**, *38*, 2017–2023. [[CrossRef](#)]
33. Parcero-Oubiña, C.; Fábrega-Álvarez, P.; Salazar, D.; Troncoso, A.; Hayashida, F.; Pino, M.; Borie, C.; Echenique, E. Ground to air and back again: Archaeological prospection to characterize prehispanic agricultural practices in the high-altitude Atacama (Chile). *Quat. Int.* **2017**, *435 Pt B*, 95–110. [[CrossRef](#)]
34. Smith, S.L.; Chambrade, M.-L. The Application of Freely-Available Satellite Imagery for Informing and Complementing Archaeological Fieldwork in the “Black Desert” of North-Eastern Jordan. *Geosciences* **2018**, *8*, 491. [[CrossRef](#)]
35. Lamenza, G. GIS and remote sensing in the archaeological research of the Argentine Chaco. *Arqueol. Iberoam.* **2015**, *27*, 40–54.
36. Dellepiane, J. Uso de imágenes satelitales para el reconocimiento de parapetos en el centro-oeste de Patagonia meridional. *Arqueología* **2018**, *24*, 259–269.
37. Bognanni, F. La teledetección aplicada al estudio del pasado a una escala inter-regional. *Rev. Española Antropol. Am.* **2010**, *40*, 77–93.
38. Binford, L.R. Organization and formation processes: Looking at curated technologies. *J. Anthropol. Res.* **1979**, *36*, 255–273. [[CrossRef](#)]
39. Kelly, R.L. The Three Sides of a Biface. *Am. Antiq.* **1988**, *53*, 717–734. [[CrossRef](#)]
40. Nelson, M. The study of technological organization. In *Archaeological Method and Theory*; Schiffer, M., Ed.; University of Arizona Press: Tucson, Arizona, 1991; pp. 57–100.
41. Roth, B.J. Mobility, Technology, and Archaic Lithic Procurement Strategies in the Tucson Basin. *Kiva* **1998**, *63*, 241–262. [[CrossRef](#)]
42. Binford, L.R. *An Archaeological Perspective*; Seminar Press: New York, NY, USA, 1972.
43. Odell, G. Economizing Behavior and the Concept of “Curation”. In *Stone Tools. Theoretical Insights into Human Prehistory*; Plenum Press: New York, NY, USA, 1996; pp. 51–80.
44. Beck, C.; Taylor, A.; Jones, G.; Fadem, C.; Cook, C.; Millward, S. Rocks are heavy: Transport costs and Paleoarchaic quarry behavior in the Great Basin. *J. Anthropol. Archaeol.* **2002**, *21*, 481–507. [[CrossRef](#)]

45. Núñez, L. Secuencia de asentamientos prehistóricos del área de Taltal. En Tres ensayos para una historia de Taltal y su zona. *Rev. Futuro* **1984**, *8*, 28–76.
46. Urrejola, C.; Orellana, M. *Explotación y Utilización de Recursos Líticos de la Zona Desértica al Interior de Tal-Tal*; Universidad de Chil: Santiago, Chile, 1999.
47. Castelletti, J. *Patrón de Asentamiento y uso de Recursos a Través de la Secuencia Ocupacional Prehispánica en la Costa de Taltal*; Universidad Católica del Norte-Universidad de Tarapacá: Arica, Chile, 2007.
48. Blanco, J.F.; de la Maza, M.; Rees, C. Cazadores Recolectores Costeros y el Aprovisionamiento de Recursos Líticos. Perspectivas Interpretativas de los Eventos de Talla en el Desierto Absoluto. *Rev. Werkén* **2010**, *13*, 45–68.
49. Pimentel, G.; Rees, C.; De Souza, P.; Arancibia, L. Viajeros costeros y caravaneros. Dos estrategias de movilidad en el Período Formativo del desierto de Atacama, Chile. In *En Ruta. Arqueología, Historia y Etnografía del tráfico Sur Andino*; Núñez, L., Nielsen, A., Eds.; Encuentro Grupo Editor: Córdoba, Argentina, 2011; pp. 43–81.
50. Salazar, D.; Figueroa, V.; Andrade, P.; Salinas, H.; Olguín, L.; Power, X.; Rebollo, S.; Parra, S.; Orellana, H.; Urrea, J. Cronología y organización económica de las poblaciones arcaicas de la costa de Taltal. *Estud. Atacameños* **2015**, *50*, 7–46. [[CrossRef](#)]
51. Power, X.; Arenas, C.; Monroy, I.; Traverso, F.; Galarce, P.; Parra, S. *Informe Lítica Proyecto Fondecyt 1151203*, Unpublished manuscript, Santiago, Chile. 2019.
52. Ballester, B.; Crisóstomo, M. Percutores de la Pampa del Desierto de Atacama (Norte de Chile): Tecnología, Huellas de Uso, Decoración y Talladores. *Chungara* **2017**, *49*, 175–192. [[CrossRef](#)]
53. Borie, C.; Power, X.; Parra, S.; Salinas, H.; Rostan, P.; Galarce, P.; Peña, I.; Traverso, F. Tras la Huella del Sílice Pampino. Nuevas Metodologías para el Rastreo de las Áreas Fuente de Aprovisionamiento lítico en Taltal. *Estud. Atacameños* **2017**, *56*, 103–131. [[CrossRef](#)]
54. Borie, C.; Salazar, D.; Power, X.; Figueroa, M.J.; Orellana, H.; Parra, S.; Arenas, C.; Traverso, F.; Monroy, I. Cazadores-Recolectores Marítimos en la Pampa Desértica de Taltal. Conocimientos, Recursos, Prácticas Sociales y Territorialización. In *Estudios de Arqueología, Historia, Filosofía y Ciencias Sociales. En Homenaje a Mario Orellana Rodríguez (60 Años de Vida Académica y Científica)*; Orellana, F., Ed.; Ediciones del Desierto: San Pedro de Atacama, Antofagasta, Chile, 2017; pp. 205–242.
55. Dunai, T.J.; González López, G.A.; Juez-Larré, J. Oligocene–Miocene Age of Aridity in the Atacama Desert Revealed by Exposure Dating of Erosion-Sensitive Landforms. *Geology* **2005**, *33*, 321–324. [[CrossRef](#)]
56. Houston, J. Variability of Precipitation in the Atacama Desert: Its Causes and Hydrological Impact. *Int. J. Climatol.* **2006**, *26*, 2181–2198. [[CrossRef](#)]
57. Placzek, C.; Quade, J.; Betancourt, J.L.; Patchett, P.J.; Rech, J.A.; Latorre, C.; Matmon, A.; Holmgren, C.; English, N.B. Climate in the dry central andes over geologic, millennial, and interannual timescales. *Ann. Mo. Bot. Gard.* **2009**, *96*, 386–397. [[CrossRef](#)]
58. Amundson, R.; Dietrich, W.; Bellugi, D.; Ewing, S.; Nishiizumi, K.; Chong, G.; Owen, J.; Finkel, R.; Heimsath, A.; Stewart, B.; et al. Geomorphologic Evidence for the Late Pliocene Onset of Hyperaridity in the Atacama Desert. *Gsa Bull.* **2012**, *124*, 1048–1070. [[CrossRef](#)]
59. Chuvieco, E. *Teledetcción Ambiental*; Ariel: Barcelona, Spain, 2006.
60. Hunt, G. Spectral Signatures of Particulate Minerals in the Visible and Near Infrared. *Geophysics* **1977**, *42*, 501–513. [[CrossRef](#)]
61. Clark, R.; King, T.; Klejwa, M.; Swayze, G.; Vergo, N. High spectral resolution reflectance spectroscopy of minerals. *J. Geophys. Res.* **1990**, *95*, 12653–12680. [[CrossRef](#)]
62. Carranza, E.J.M.; Hale, M. Mineral imaging with Landsat Thematic Mapper data for hydrothermal alteration mapping in heavily vegetated terrane. *Int. J. Remote Sens.* **2002**, *23*, 4827–4852. [[CrossRef](#)]
63. Cattáneo, R.; Di Lello, C.; Gómez, J.C. Cuantificación y análisis de la distribución de rocas útiles para la manufactura de instrumentos a través del uso de Sistemas de Información Geográfica (SIG) en el área de Piedra Museo, Santa Cruz, Argentina. In *El uso de Sistemas de Información Geográfica en Arqueología Sudamericana*; Figueroa, M.J., Izeta, A., Eds.; Archaeopress: Oxford, UK, 2013; pp. 43–60.
64. Goudie, A.S. *Arid and Semi-Arid Geomorphology*; Cambridge University Press: New York, NY, USA, 2013.
65. Ortlieb, L.; Vargas, G.; Saliége, J. Marine radiocarbon reservoir effect along the northern Chile–southern Peru coast (14–24°S) throughout the Holocene. *Quat. Res.* **2011**, *75*, 91–103. [[CrossRef](#)]

66. Marquet, P.A.; Bozinovic, F.; Bradshaw, G.A.; Cornelius, C.; González, H.; Gutiérrez, J.R.; Hajek, E.R.; Lagos, J.A.; López-Cortes, F.; Núñez, L.; et al. Los Ecosistemas del Desierto de Atacama y Área Andina Adyacente en el Norte de Chile. *Rev. Chil. Hist. Nat.* **1998**, *71*, 593–617.
67. Vargas, G.; Ruttlant, J.; Ortlieb, L. ENSO Tropical–Extratropical Climate Teleconnections and Mechanisms for Holocene Debris Flows Along the Hyperarid Coast of Western South America ( $17^{\circ}$ – $24^{\circ}$ S). *Earth Planet. Sci. Lett.* **2006**, *249*, 467–483. [[CrossRef](#)]
68. Herrera, C.; Custodio, E. Origin of waters from small springs located at the northern coast of Chile, in the vicinity of Antofagasta. *Andean Geol.* **2014**, *41*, 314–341.
69. Placzek, C.; Matmon, A.; Granger, D.; Quade, J.; Niedermann, S. Evidence for active landscape evolution in the hyperarid Atacama from multiple terrestrial cosmogenic nuclides. *Earth Planet. Sci. Lett.* **2010**, *295*, 12–20. [[CrossRef](#)]
70. Gajardo, R. *La Vegetación Natural de Chile: Clasificación y Distribución Geográfica*; Editorial Universitaria: Santiago, Chile, 1994.
71. Clarke, J.D.A. Antiquity of Aridity in the Chilean Atacama Desert. *Geomorphology* **2006**, *73*, 101–114. [[CrossRef](#)]
72. Quade, J.; Rech, J.A.; Betancourt, J.; Latorre, C.; Quade, B.; Rylander, K.A.; Fisher, T. Paleowetlands and Regional Climate Change in the Central Atacama Desert, Northern Chile. *Quat. Res.* **2008**, *69*, 343–360. [[CrossRef](#)]
73. Gayó, E.M.; Latorre, C.; Jordán, T.; Nester, P.; Estay, S.; Ojeda, C.; Santoro, C. Late Quaternary Hydrological and Ecological Changes in the Hyperarid Core of the Northern Atacama Desert ( $\sim 21^{\circ}$ S). *Earth-Sci. Rev.* **2012**, *113*, 120–140.
74. Sáez, A.; Godfrey, L.V.; Herrera, C.; Chong, G.; Pueyo, J.J. Timing of Wet Episodes in Atacama Desert over the Last 15 ka. The Groundwater Discharge Deposits (GWD) from Domeyko Range at  $25^{\circ}$ S. *Quat. Sci. Rev.* **2016**, *145*, 82–93. [[CrossRef](#)]
75. Santoro, C.M.; Capriles, J.M.; Gayo, E.M.; de Porras, M.E.; Maldonado, A.; Standen, V.G.; Latorre, C.; Castro, V.; Angelo, D.; McRostie, V.; et al. Continuities and Discontinuities in the Socio-Environmental Systems of the Atacama Desert During the Last 13,000 years. *J. Anthropol. Archaeol.* **2017**, *46*, 28–39. [[CrossRef](#)]
76. Pfeiffer, M.; Latorre, C.; Santoro, C.M.; Gayo, E.M.; Rojas, R.; Carrevedo, M.L.; McRostie, V.B.; Finstad, K.M.; Heimsath, A.; Jungers, M.C.; et al. Chronology, Stratigraphy and Hydrological Modelling of Extensive Wetlands and Paleolakes in the Hyperarid Core of the Atacama Desert During the Late Quaternary. *Quat. Sci. Rev.* **2018**, *197*, 224–245. [[CrossRef](#)]
77. Llagostera, A. 9,700 Years of Maritime Subsistence on the Pacific: An Analysis by Means of Bioindicators in the North of Chile. *Am. Antiq.* **1979**, *44*, 309–324. [[CrossRef](#)]
78. Ballester, B.; Gallardo, F. Prehistoric and historic networks on the Atacama Desert coast (northern Chile). *Antiquity* **2011**, *85*, 875–889. [[CrossRef](#)]
79. Luedtke, B.E. *An Archaeologist's Guide to Chert and Flint*; Institute of Archaeology, University of California: Los Angeles, CA, USA, 1992.
80. Naranjo, J.; Puig, A. *Carta Geológica de Chile escala 1:250.000. Hojas Taltal y Chañaral N°62 y 63*; Servicio Nacional de Geología y Minería: Santiago, Chile, 1984.
81. Marinovic, N.; Smoje, I.; Makasev, V.; Hervé, M.; Mpodozis, C. *Carta Geológica de Chile Escala 1:250.000. Hoja Aguas Blancas, Región de Antofagasta*; Servicio Nacional de Geología y Minería: Santiago, Chile, 1995.
82. Sernageomin. *Mapa Geológico de Chile: Versión Digital*; Servicio Nacional de Geología y Minería: Santiago, Chile, 2003.
83. Rech, J.A.; Latorre, C. Climatic Controls on Fluvial Cut-and-Fill Cycles in Drainages with in-Stream Wetlands in the Central Andes. In Proceedings of the American Geophysical Union, Fall Meeting, San Francisco, CA, USA, 13–17 December 2004. Abstract-H51A-1103.
84. Kober, F.; Ivy-Ochs, S.D.; Schlunegger, F.; Baur, H.; Kubik, P.W.; Wieler, R. Denudation Rates and a Topography-Driven Rainfall Threshold in Northern Chile: Multiple Cosmogenic Nuclide Data and Sediment Yield Budgets. *Geomorphology* **2007**, *83*, 97–120. [[CrossRef](#)]
85. Xiong, Y.; Shuhab, K.; Khalid, M.; Sisson, V. Lithological mapping of Bela ophiolite with remote-sensing data: International. *J. Remote Sens.* **2011**, *32*, 4641–4658. [[CrossRef](#)]
86. Pour, A.B.; Hashim, M. Hydrothermal alteration mapping from Landsat-8 data, Sar Cheshmeh copper mining district, south-eastern Islamic Republic of Iran. *J. Taibah Univ. Sci.* **2015**, *9*, 155–166. [[CrossRef](#)]

87. Abrams, M.J.; Ashley, R.P.; Rowan, L.C.; Goetz, A.F.H.; Kahle, A.B. Mapping of hydrothermal alteration in the Cuprite mining district, Nevada, using aircraft scanner images for the spectral region 0.46 to 2.36 $\mu$ m. *Geology* **1977**, *5*, 713–718. [[CrossRef](#)]
88. Gad, S.; Kusky, T. ASTER spectral ratioing for lithological mapping in the Arabian–Nubian shield, the Neoproterozoic Wadi Kid area, Sinai, Egypt. *Gondwana Res.* **2007**, *11*, 326–335. [[CrossRef](#)]
89. Lillesand, T.; Kiefer, R.; Chipman, J. *Remote Sensing and Image Interpretation*, 6th ed.; John Wiley & Sons Ltd.: Hoboken, NJ, USA, 2008; p. 736.
90. Catella, L.; Barrientos, G.; Oliva, F. La identificación del uso de fuentes secundarias de materiales líticos asistida por SIG: El Arroyo Chasicó (Argentina) como caso de estudio. *Estud. Geol.* **2017**, *73*, 1–20. [[CrossRef](#)]
91. Magnin, L.A. Hunter-gatherer provisioning strategies in a landscape with abundant lithic resources (La Primavera, Santa Cruz, Argentina). *Quat. Int.* **2015**, *375*, 55–71. [[CrossRef](#)]
92. Skarbun, F. Estructura y explotación de los recursos líticos en el sector Meridional de la Meseta Central de Santa Cruz, Argentina. *Magallania (Punta Arenas)* **2015**, *43*, 191–209. [[CrossRef](#)]
93. Clarkson, C.; Bellas, A. Mapping stone: Using GIS spatial modelling to predict lithic source zones. *J. Archaeol. Sci.* **2014**, *46*, 324–333. [[CrossRef](#)]
94. Duke, C.; Steele, J. Geology and lithic procurement in Upper Palaeolithic Europe: A weights-of-evidence based GIS model of lithic resource potential. *J. Archaeol. Sci.* **2010**, *37*, 813–824. [[CrossRef](#)]
95. Clarke, K.D. *Geología, Petrografía y Geoquímica de las Rocas Intrusivas de la Cordillera de la Costa entre Paposo y Taltal. Memoria para Optar al Título de Geólogo*; Facultad de Ingeniería y Ciencias Geológicas, Departamento de Ciencias Geológicas, Universidad Católica del Norte: Antofagasta, Chile, 1998.
96. Galarce, P.; Santander, G. Contextos líticos de asentamientos arcaicos en la costa de Taltal (II Región, Chile). *Estud. Atacameños* **2013**, *46*, 5–26. [[CrossRef](#)]
97. Warner, T.A.; Campagna, D.J. *Remote Sensing with IDRISI Taiga: A Beginner's Guide*; Geocarto International Centre: Hong Kong, China, 2009.
98. Ali, A.; Pour, A.B. Lithological mapping and hydrothermal alteration using Landsat 8 data: A case study in arriab mining district, red sea hills, Sudan. *Int. J. Basic Appl. Sci.* **2014**, *3*, 199–208. [[CrossRef](#)]
99. Rowan, L.C.; Schmidt, R.G.; Mars, J.C. Distribution of hydrothermally altered rocks in the Reko Diq, Pakistan mineralized area based on spectral analysis of ASTER data. *Remote Sens. Environ.* **2006**, *104*, 74–87. [[CrossRef](#)]
100. Pour, A.B.; Hashim, M. The application of ASTER remote sensing data to porphyry copper and epithermal gold deposits. *Ore Geol. Rev.* **2012**, *44*, 1–9. [[CrossRef](#)]
101. Mars, J.C.; Rowan, L.C. Spectral assessment of new ASTER SWIR surface reflectance data products for spectroscopic mapping of rocks and minerals. *Remote Sens. Environ.* **2010**, *114*, 2011–2025. [[CrossRef](#)]
102. Watanabe, H.; Matsuo, K. Rock type classification by multi-band TIR of ASTER. *Geosci. J.* **2003**, *7*, 347–358. [[CrossRef](#)]
103. Shackley, M.S. Archaeological Petrology and the Archaeometry of Lithic Materials. *Archaeometry* **2008**, *50*, 194–215. [[CrossRef](#)]
104. Andrefsky, W. The Analysis of Stone Tool Procurement, Production, and Maintenance. *J. Archaeol. Res.* **2009**, *17*, 65–103. [[CrossRef](#)]
105. Parish, R.M. The Application of Visible/Near-Infrared Reflectance (VNIR) Spectroscopy to Chert: A Case Study from the Dover Quarry Sites, Tennessee. *Geoarchaeology* **2011**, *26*, 420–439. [[CrossRef](#)]
106. Wilson, L. Understanding prehistoric lithic raw material selection: Application of a gravity model. *J. Archaeol. Method Theory* **2007**, *14*, 388–411. [[CrossRef](#)]
107. Monroy, I.; Borie, C.; Troncoso, A.; Power, X.; Parra, S.; Galarce, P.; Pino, M. Navegantes del desierto. Un nuevo sitio con arte rupestre estilo El Médano en la Depresión Intermedia de Taltal. *Taltalia* **2016**, *27*–48. [[CrossRef](#)]

